

RESEARCH ARTICLE

FGF signaling in mammary gland fibroblasts regulates multiple fibroblast functions and mammary epithelial morphogenesis

Jakub Sumbal and Zuzana Koledova*

ABSTRACT

Fibroblast growth factor (FGF) signaling is crucial for mammary gland development. Although multiple roles for FGF signaling in the epithelium have been described, the function of FGF signaling in mammary stroma has not been elucidated. In this study, we investigated FGF signaling in mammary fibroblasts. We found that murine mammary fibroblasts express FGF receptors FGFR1 and FGFR2 and respond to FGF ligands. In particular, FGF2 and FGF9 induce sustained ERK1/2 signaling and promote fibroblast proliferation and migration in 2D cultures. Intriguingly, only FGF2 induces fibroblast migration in 3D extracellular matrix (ECM) through regulation of actomyosin cytoskeleton and promotes force-mediated collagen remodeling by mammary fibroblasts. Moreover, FGF2 regulates production of ECM proteins by mammary fibroblasts, including collagens, fibronectin, osteopontin and matrix metalloproteinases. Finally, using organotypic 3D co-cultures we show that FGF2 and FGF9 signaling in mammary fibroblasts enhances fibroblast-induced branching of mammary epithelium by modulating paracrine signaling, and that knockdown of *Fgfr1* and *Fgfr2* in mammary fibroblasts reduces branching of mammary epithelium. Our results demonstrate a pleiotropic role for FGF signaling in mammary fibroblasts, with implications for regulation of mammary stromal functions and epithelial branching morphogenesis.

KEY WORDS: Branching morphogenesis, Collagen, Extracellular matrix, Fibroblast, Fibroblast growth factor, Mammary gland, Stroma, Mouse

INTRODUCTION

Fibroblast growth factor (FGF) signaling is a crucial pathway that regulates vertebrate development from the earliest embryonic stages throughout the animal's lifetime (Turner and Grose, 2010). Importantly, FGF signaling has a conserved role in the regulation of branching morphogenesis, governing development of branched organs such as fly trachea and mammalian lung, salivary gland, kidney and mammary gland (Affolter et al., 2009; Lu and Werb, 2008). In mammals, FGF signaling comprises 22 FGF ligands, 18 of which act through four transmembrane tyrosine kinase receptors (FGFR1–FGFR4). Ligand-binding specificity of FGFR1–FGFR3 is generated by alternative splicing of the extracellular immunoglobulin domain III, creating IIIb and IIIc variants of FGFR1–FGFR3. Binding of an FGF ligand to FGFR requires a co-factor (heparan sulfate) and results in receptor dimerization, phosphorylation and

activation of downstream signaling pathways, including Ras-MEK-ERK, PI3K-AKT, PLC γ and STAT3 signaling pathways (Turner and Grose, 2010).

FGF signaling is essential for normal mammary gland development. Loss of *Fgf10* or its receptor *Fgfr2* results in a failure to form mammary placodes during embryogenesis (Kim et al., 2013; Mailleux et al., 2002). Conditional deletion of epithelial *Fgfr1* or *Fgfr2* results in transient developmental defects in branching morphogenesis (Lu et al., 2008; Parsa et al., 2008; Pond et al., 2013), whereas simultaneous deletion of both *Fgfr1* and *Fgfr2* in the mammary epithelium compromises mammary stem cell activities (Pond et al., 2013). Several FGF ligands are produced by the pubertal mammary gland stroma, including FGF2, FGF7, FGF9 and FGF10, and regulate distinct aspects of epithelial morphogenesis (Zhang et al., 2014b). However, the role of FGF signaling in mammary stroma has not been elucidated.


Mammary stroma consists of extracellular matrix (ECM) and several cell types, including fibroblasts, adipocytes, immune and endothelial cells, and has an instructive role in regulating mammary gland development (Nelson and Bissell, 2006; Wiseman and Werb, 2002). Through providing paracrine signals, mechanical cues and organization of the 3D ECM scaffold, mammary stroma guides mammary epithelial branching morphogenesis from embryonic stage throughout puberty, epithelial differentiation to milk-producing alveoli during lactation and epithelial remodeling during involution (Polyak and Kalluri, 2010; Schedin and Hovey, 2010).

The important role of fibroblasts in modulating mammary epithelial response was described more than 30 years ago (Haslam, 1986), yet the mechanisms of action of fibroblasts in mammary gland development have only recently started to be revealed. In 3D co-cultures in collagen, fibroblasts induced formation of invasive branched mammary epithelial structures through paracrine hepatocyte growth factor signaling (Zhang et al., 2002). Fibroblasts were found to be essential for formation of mammary epithelial ductal structures upon transplantation of human mammary organoids into humanized mouse fat pads (Kuperwasser et al., 2004) and in 3D co-culture of MCF10A cells (Krause et al., 2008). Genetic mouse models demonstrated the essential roles of fibroblast-mediated paracrine signaling and ECM remodeling in mammary gland development (Hammer et al., 2017; Jones et al., 2019; Koledova et al., 2016; Peuhu et al., 2017) and revealed regulation of these functions by receptor tyrosine kinase signaling, including platelet-derived growth factor receptor (PDGFR) and EGFR-ERK1/2 pathways (Hammer et al., 2017; Koledova et al., 2016).

In this study, we investigated FGF signaling in mammary fibroblasts and its implications for mammary gland development using 2D and 3D cultures of primary mammary fibroblasts. We present our findings on the components and activity of FGF signaling in mammary fibroblasts, and the roles of FGF signaling in regulation of fibroblast

Department of Histology and Embryology, Faculty of Medicine, Masaryk University, Kamenice 3, Brno 625 00, Czech Republic.

*Author for correspondence (koledova@med.muni.cz)

 J.S., 0000-0003-3700-4518; Z.K., 0000-0002-9333-1399

Received 3 October 2019; Accepted 24 October 2019

proliferation, migration, ECM production and remodeling, and fibroblast-mediated mammary epithelial branching morphogenesis.

RESULTS

FGFR1 and FGFR2 are expressed in mammary fibroblasts

To investigate the FGF signaling machinery in mammary fibroblasts, we isolated fibroblasts as well as epithelial organoids from mammary glands of pubertal mice and we analyzed expression of FGFR variants (genes *Fgfr1-Fgfr4* and their variants IIIb and IIIc, further referred to as 'b' or 'c') in these cell populations using qPCR. The purity of cell populations was checked by expression of the epithelial marker gene *Cdh1* and mesenchymal marker gene *Vim* (Fig. 1A). We detected expression of a wide range of *Fgfr* genes in mammary epithelium, including *Fgfr1b*, *Fgfr1c*, *Fgfr2b*, *Fgfr3b*, *Fgfr3c* and *Fgfr4*. However, in mammary fibroblasts, only *Fgfr1c* and *Fgfr2c* were expressed (Fig. 1A).

To test expression of FGFR1 and FGFR2 proteins in fibroblasts, we performed immunohistochemical staining of mammary gland tissue (Fig. 1B) and immunofluorescent staining of mammary fibroblasts in culture (Fig. 1C,D). Fibroblasts in mammary gland tissue sections, identified as spindle shaped-cells surrounding the epithelium, expressed both FGFR1 and FGFR2 (Fig. 1B). Similarly, primary fibroblasts cultured *in vitro* in 2D, positive for fibroblast markers PDGFR α and vimentin (Fig. S1A), expressed both FGFR1 and FGFR2. FGFR1 was localized mostly to the plasma membrane and cytoplasm (Fig. 1C), including Golgi apparatus (Fig. S1B). FGFR2 appeared to be predominantly localized to the nucleus or perinuclear region of cytoplasm (Fig. 1C) and only a small fraction of FGFR2 colocalized with the Golgi apparatus marker GM130 (Fig. S1B). When the fibroblasts were cultured in 3D in Matrigel, both FGFR1 and FGFR2 were localized in the cell membrane, cytoplasm and nucleus (Fig. 1D).

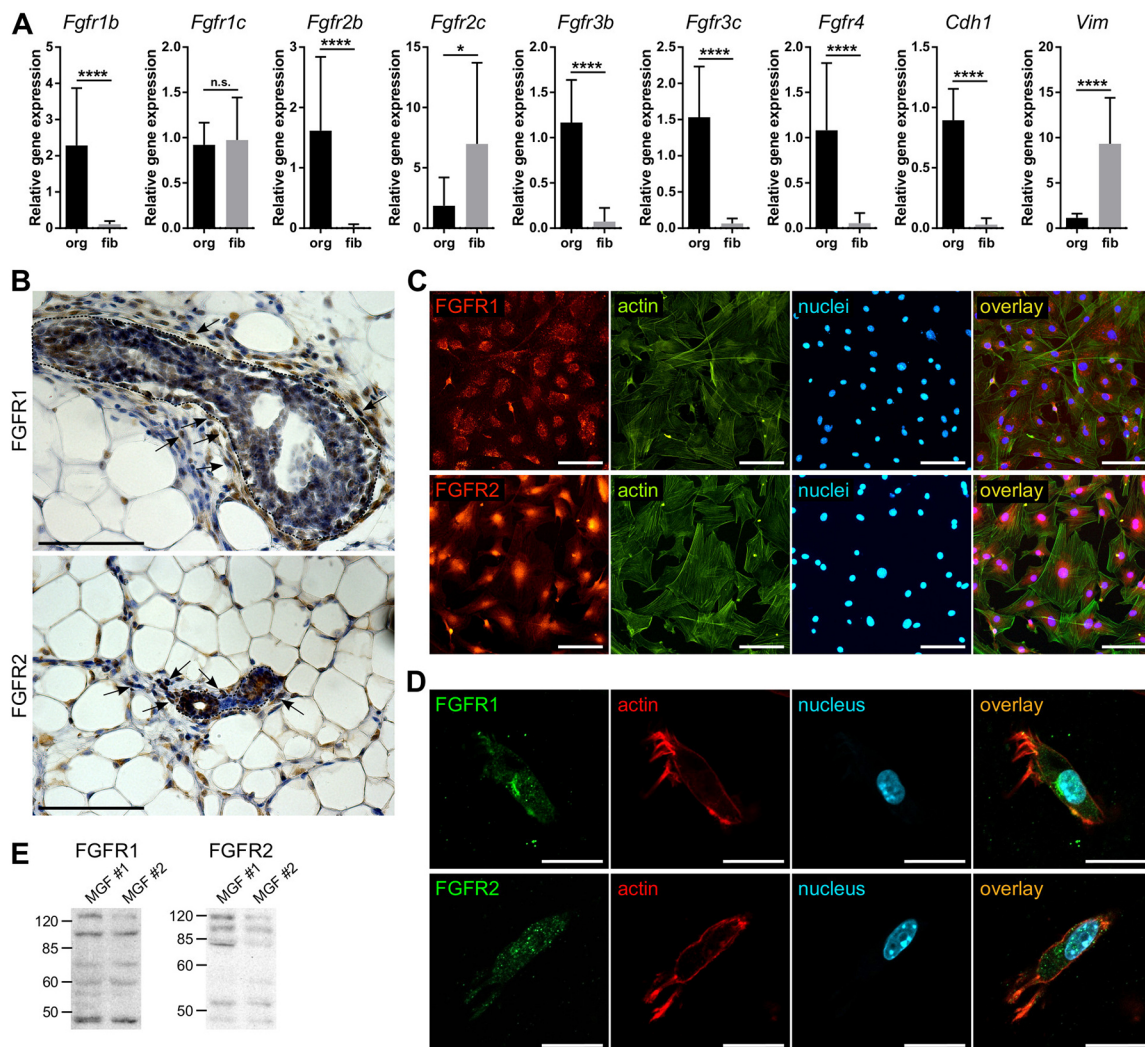


Fig. 1. Mammary fibroblasts express FGFR1 and FGFR2 and respond to FGF ligands. (A,B) Analysis of FGFR expression in mammary fibroblasts. (A) Relative expression of *Fgfr* gene variants in mammary fibroblasts, compared with mammary epithelial organoids. Data are mean \pm s.d., $n=9$ organoid and 22 fibroblast samples. * $P < 0.05$; **** $P < 0.0001$ (unpaired Student's *t*-test). n.s., not significant. (B) Detection of FGFR1 and FGFR2 in whole-mount mammary gland by immunohistochemistry. Dotted lines encircle mammary epithelium. Arrows indicate some of the fibroblasts. Note expression of both FGFR1 and FGFR2 in mammary fibroblasts as well as epithelium. Blue indicates nuclei stained by hematoxylin. Scale bars: 100 μ m. (C,D) Detection of FGFR1 and FGFR2 in primary mammary fibroblasts by immunofluorescence. The fibroblasts were cultured in 2D on glass coverslips (C) or in 3D Matrigel (D). Actin was stained with phalloidin, nuclei were stained with DAPI. Scale bars: 100 μ m in C; 20 μ m in D. (E) Western blot analysis of FGFR1 and FGFR2 in two samples of primary mammary gland fibroblasts (MGF). The numbers and lines indicate protein molecular weight markers (in kDa).

Western blot analysis of mammary fibroblasts (cultured in 2D) detected FGFR1 and FGFR2 proteins in both full length as well as their truncated fragments (Fig. 1E). These truncated fragments could represent the nuclear fraction of the receptors (Chioni and Grose, 2012) and thus support our results from immunofluorescence on nuclear FGFRs.

FGF ligands induce activation of intracellular signaling pathways downstream of FGFR in mammary fibroblasts

Next we tested four FGF ligands – FGF2, FGF7, FGF9 and FGF10 – which were reported to be expressed in pubertal mammary gland (Zhang et al., 2014b), for their ability to induce FGFR signaling in mammary fibroblasts. To this end, we investigated activation of the main signaling pathways downstream of FGFR, ERK1/2 and AKT, using western blot detection of activated (phosphorylated) forms of ERK1/2 and AKT after addition of FGF ligands to serum-starved fibroblasts. We found that all four FGF ligands induced phosphorylation of ERK1/2 and AKT 5 min after FGF treatment (Fig. 2A-C). However, only in response to FGF2 or FGF9, ERK1/2 phosphorylation (and AKT phosphorylation in the case of FGF2) was sustained beyond 5 min and displayed typical dynamics, with signaling at maximum levels at 5 min, followed by a gradual decrease of phosphorylation for 60 min after FGF treatment. Activation of ERK1/2 and AKT after FGF7 or FGF10 treatment was only transient and diminished within 15 min of FGF treatment. Therefore, FGF7 and FGF10 were unlikely to induce a cellular response.

FGF2 and FGF9 regulate mammary fibroblast proliferation and migration

In many cell types, FGF signaling is an important regulator of cell proliferation and survival. Therefore, we tested the importance of FGF signaling in mammary fibroblast proliferation and survival

using two FGFR inhibitors: BGJ398 (Guagnano et al., 2011) and SU5402 (Sun et al., 1999). We found that both FGFR inhibitors efficiently inhibit fibroblast proliferation and/or survival in a dose- and cell density-dependent manner (Fig. S2A,B). The half maximal inhibitory concentration (IC_{50}) of BGJ398 was 6.98 nM for less confluent cells, and 11.41 nM for more confluent cells. The IC_{50} of SU5402 was 284 nM and 1110 nM for less and more confluent cells, respectively.

Encouraged by the results from FGFR inhibitor assays that suggested that FGF signaling plays a role in fibroblast proliferation and survival, we tested FGF ligands for their effects on fibroblasts. Using MTT and resazurin proliferation assays, we found that in both 2D and 3D culture conditions, FGF2 and FGF9 enhanced fibroblast proliferation, whereas FGF7 and FGF10 did not (Fig. 3A,B, Fig. S2C).

Next, we tested the effect of FGF ligands on fibroblast migration in 2D using two different assays: scratch assay (or wound healing assay) and transwell migration assay. In the transwell migration assay, we tested the capacity of different FGF ligands to induce directed fibroblast migration: from one side of a porous membrane in medium with no FGF (upper well), to the other side of the membrane with medium supplemented with different FGF ligands (bottom well). We observed increased migration of fibroblasts towards the medium with FGF2 and FGF9 (Fig. 3C). FGF7 and FGF10 did not act as chemoattractants for the fibroblasts (Fig. 3C).

In the scratch assay, fibroblasts were cultured to confluence and then serum-starved to silence growth factor signaling and to stop cell proliferation. Next, the cell covered area was scratched to remove cells and to create a cell-free zone, into which the cells can migrate by non-directional migration. We found that fibroblasts migrated into the scratch area even without any FGF in the medium. FGF2 and FGF9 significantly enhanced fibroblast migration,

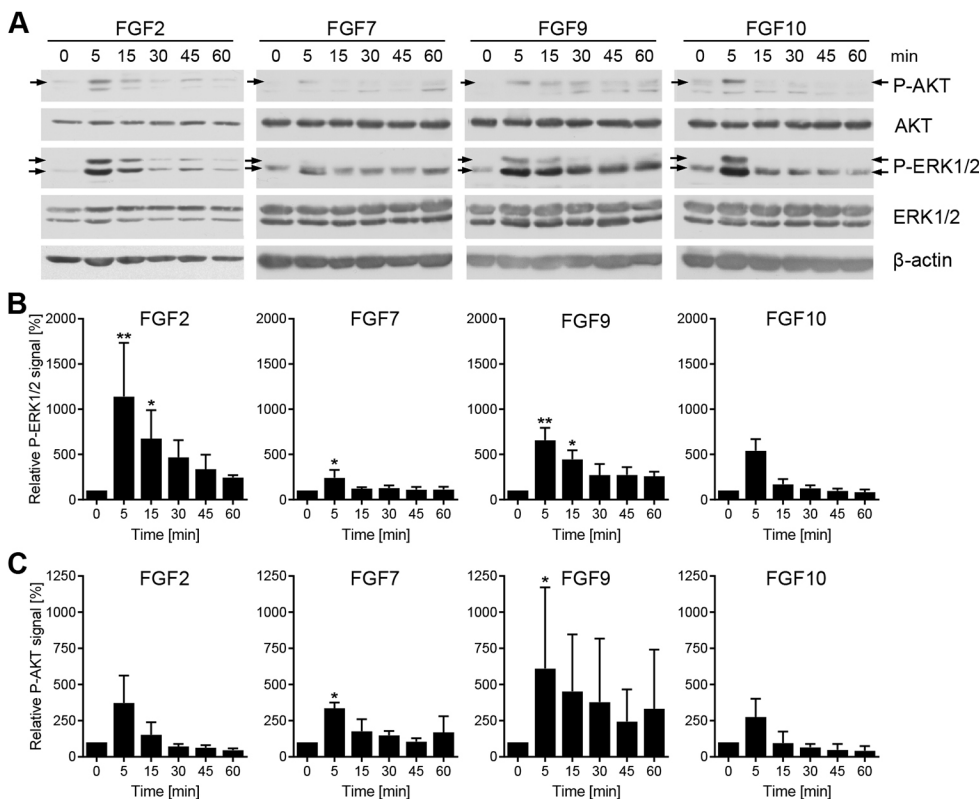


Fig. 2. Investigation of activation of ERK1/2 and AKT signaling pathways in response to FGF ligands using western blot. (A) Representative western blots for FGF2, FGF7, FGF9 and FGF10. Arrows show positions of P-AKT and P-ERK1/2 bands on the blot. (B,C) Quantification of P-ERK1/2 signal, normalized to ERK1/2 (B) or P-AKT signal, normalized to AKT (C). Data are mean+s.d., $n=3$. * $P<0.05$; ** $P<0.01$ [Friedman test, change in comparison with cells not treated with FGF (time point 0 min)].

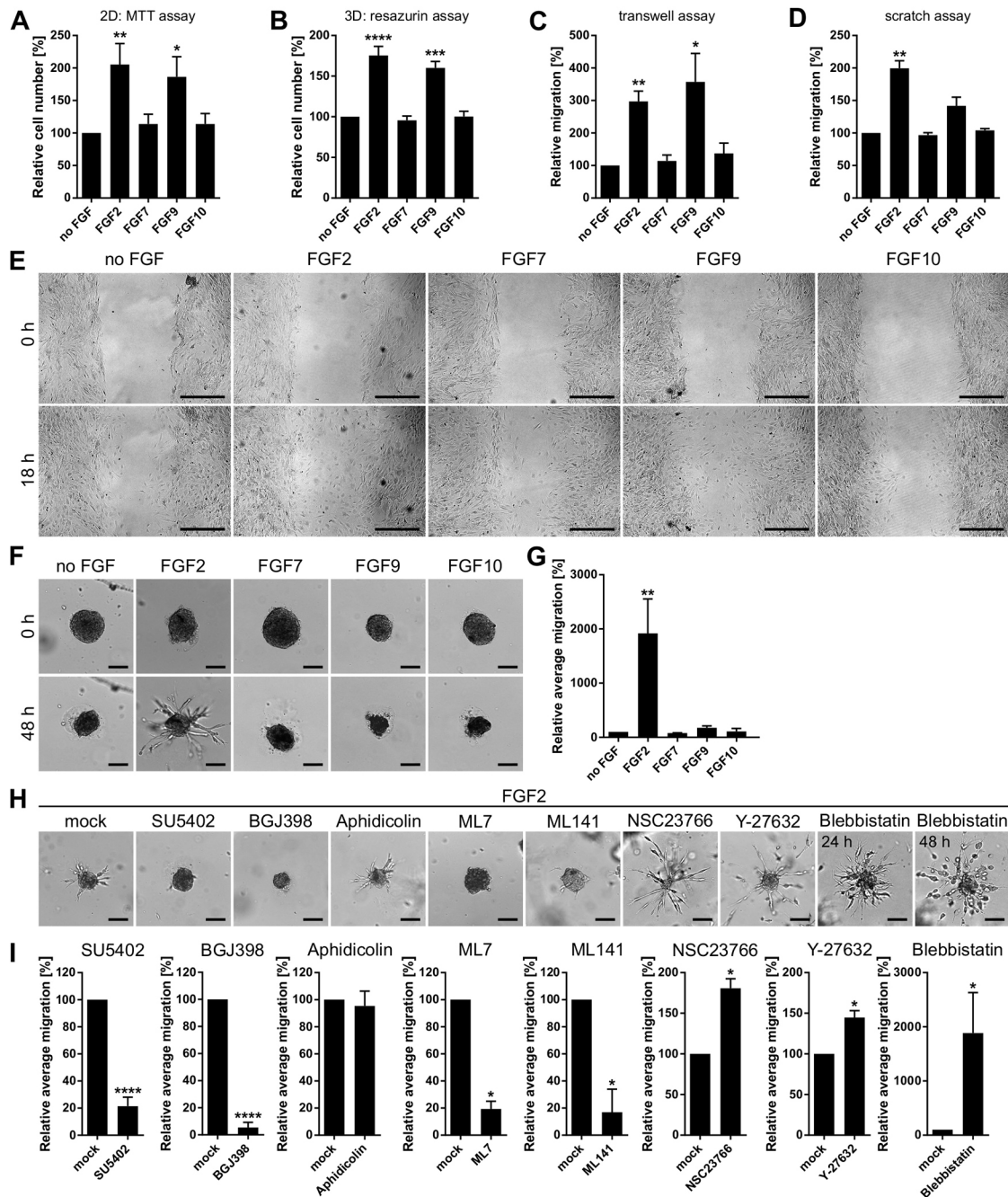


Fig. 3. FGF signaling regulates fibroblast proliferation and migration. (A,B) FGF proliferation assays in 2D using MTT assay (A) and in 3D using resazurin assay (B). Data are mean+s.d., $n=4-8$ (A), $n=3$ (B). * $P<0.05$; ** $P<0.01$; *** $P<0.001$; **** $P<0.0001$ (Kruskal–Wallis test in A; one-way ANOVA in B; change in comparison with cells with no FGF). (C) Transwell migration assay. Data are mean+s.d., $n=3-7$. * $P<0.05$; ** $P<0.01$ (Kruskal–Wallis test). (D,E) Quantification of scratch assay (D) and representative photographs of scratch areas at the beginning (0 h) and end of the assay (18 h after scratch) (E). The bars represent mean+s.d., $n=3-5$. ** $P<0.01$ (Kruskal–Wallis test, change in comparison with cells with no FGF). Scale bars: 100 μm . (F–I) Fibrosphere 3D migration assay. FGF2 induces fibroblast migration in Matrigel (F,G). Representative images of fibrospheres at 0 h and 48 h (F). Scale bars: 50 μm . Quantification (G) shows average migration as mean+s.d., $n=2-4$. ** $P<0.01$ (one-way ANOVA). (H,I) FGF2-induced migration in 3D is susceptible to inhibitors of FGFR (BGJ398, SU5402), MLCK (ML7) or Cdc42 (ML141), refractory to inhibition of proliferation (aphidicolin) and potentiated by inhibitors of ROCK (Y-27632), RAC1 (NSC23766) or myosin II (blebbistatin). Representative images (H) of fibrospheres at 48 h of treatment (also at 24 h for blebbistatin). Scale bars: 50 μm . Quantification of fibroblast migration (I), shown as mean+s.d., $n=2-4$. * $P<0.05$; **** $P<0.0001$ (Student's t -test).

whereas FGF7 and FGF10 did not increase fibroblast migration over the baseline (Fig. 3D,E). Because FGF2 and FGF9 are potent inducers of fibroblast proliferation, we tested whether proliferation contributed to the wound closure in the scratch assay using mitomycin C and aphidicolin, inhibitors of DNA replication. We found that even when cell proliferation was blocked, FGF2 and

FGF9 increased wound closure (Fig. S2D,E), confirming that FGF2 and FGF9 promote wound closure via fibroblast migration.

FGF2 regulates mammary fibroblast migration in 3D ECM

Subsequently we tested the ability of FGF ligands to induce fibroblast migration in 3D ECM. We employed a fibrosphere 3D migration

assay: Fibroblasts were aggregated into a spheroid (fibrosphere), embedded in 3D Matrigel and treated with different FGF ligands. We found that FGF2 was the only one of the FGF ligands tested that effectively induced fibroblast migration in 3D Matrigel, visible as radial protrusions of spindle-shaped cells coming out from the fibrosphere in streaks (Fig. 3F,G, Fig. S2F). The migrating cells showed positive staining for both FGFR1 and FGFR2 (Fig. S2G).

We analyzed the mechanism of FGF2-induced 3D migration more deeply using specific inhibitors. We confirmed that it was FGFR dependent because FGFR inhibitors BGJ398 and SU5402 efficiently abrogated it (Fig. 3H,I, Fig. S2F). We also found out that the migration in 3D did not require fibroblast proliferation because DNA polymerase inhibitor aphidicolin did not affect it (Fig. 3H,I). Because contraction of the actomyosin cytoskeleton is crucial for cell migration, we tested the requirement for several proteins involved in regulation of cytoskeleton contractility. We observed that FGF2-induced 3D migration was efficiently inhibited by the Cdc42 inhibitor ML141 or the myosin light chain kinase (MLCK) inhibitor ML7, but enhanced by RAC1 inhibitor NSC23766 or Rho-associated protein kinase (ROCK) inhibitor Y-27632 (Fig. 3H,I, Fig. S2E). Interestingly, blebbistatin, an inhibitor of myosin II, increased cell migration in 3D ECM and it also changed the mode of cell migration to a more amoeboid-like migration, characterized by a rounded cell body with thin protrusions and decreased migration in streaks (Fig. 3H,I).

FGF2 promotes collagen remodeling by mammary fibroblasts

During mammary branching morphogenesis, the pattern of collagen fibers in ECM helps to guide mammary ductal outgrowth (Brownfield et al., 2013; Hovey et al., 2002; Ingman et al., 2006; Peuhu et al., 2017). Fibroblasts generate traction forces and reorganize collagen fibers through interaction with ECM and cell migration in response to mechanical and chemical cues (Grinnell and Petroll, 2010; Tschumperlin, 2013). Because our results demonstrated the role for FGF2 in fibroblast migration in 3D ECM (Fig. 3F,G), we investigated the role of FGF signaling in force-mediated collagen remodeling by mammary fibroblasts using a collagen contraction assay. Mammary fibroblasts were embedded in floating collagen gels and cultured with FGF ligands or serum, and the extent of collagen remodeling was assessed by the decrease of the collagen gel size. The gels with fibroblasts that were not exposed to any FGF showed a small contraction (Fig. 4A,B). FGF2 induced significant collagen gel contraction, whereas FGF7, FGF9 and FGF10 did not (Fig. 4A,B). FGF2-induced gel contraction was abrogated by FGFR inhibitors BGJ398 or SU5402 but it was refractory to aphidicolin, an inhibitor of cell proliferation (Fig. 4A,C). Inhibitors PP2, NSC23766, Y-27632, blebbistatin, or a combination of RhoA and Y16 inhibited FGF2-induced gel contraction, demonstrating that generation of mechanical force efficient to reorganize collagen required Src, RAC1, ROCK, myosin II and RhoA, respectively. Inhibitors of matrix metalloproteinases (MMPs) or lysyl oxidase (LOX) (GM6001 and BAPN, respectively) did not abrogate FGF2-induced collagen gel contraction (Fig. 4A,C).

FGF2 regulates ECM production by mammary fibroblasts

Fibroblasts are the main producers of ECM in most tissues. Therefore, we investigated the role of FGF signaling in mammary fibroblasts in ECM production. Because our previous tests showed that from the FGFs tested, FGF2 is the most potent regulator of multiple functions in mammary fibroblasts, we investigated only the effects of FGF2 on ECM production. To this end, fibroblasts were cultured in conditions that favor ECM production, at high

confluence and with L-ascorbic acid-supplemented medium. In these cultures, we analyzed the expression of candidate genes involved in ECM production using qPCR, and the ECM produced by fibroblasts was investigated using chromogenic assays, immunofluorescence and scanning electron microscopy.

The qPCR analysis revealed that FGF2 decreased expression of collagen genes *Colla1*, *Colla2* and *Col3a1*, upregulated *Col7a1*, but had no significant effect on *Col4a1* or *Col4a2* expression (Fig. 4D). Furthermore, FGF2 decreased expression of *Mmp11* and increased expression of *Timp1* (Fig. 4D) but no significant change in *Lox*, *Lox3* or *Mmp3* was detected (Fig. 4D, Figs S3 and S4). FGF2 also induced expression of fibronectin (*Fn1*) and osteopontin (*Spp1*) (Fig. 4D), but had no significant effect on expression of heparan sulfate proteoglycan (HSPG) genes *Hspg2*, *Sdc1*, *Sdc2*, *Sdc3* or *Sdc4* (Figs S3 and S4). Expression of hyaluronan synthase genes *Has2* and *Has3* was downregulated by FGF2 (Fig. 4D). Furthermore, we also detected increased expression of transforming growth factor beta 1 (*Tgfb1*), a major regulator of ECM, and *Dusp6*, an FGFR-ERK signaling target gene, and decreased expression of *Acta2*, a myofibroblast marker (Fig. 4D).

Picosirius Red staining of fibroblast ECM cultures revealed the presence of fibrillar collagen in the ECM (Fig. 5A). The amount of collagen in cultures treated with FGF2 was significantly lower than that seen in control cultures treated with serum, which were cultured to demonstrate the full potential of fibroblasts to produce ECM in these *in vitro* conditions. FGFR inhibitor (provided at low concentration to avoid cell death) had a small to negligible effect on the amount of collagen in the serum-treated cultures, demonstrating that signaling pathways other than the FGF pathway are the main regulators of collagen production and deposition in serum-treated cultures. When compared with cultures with no FGF, the FGF2-treated cultures appeared to contain a similar amount of collagen (Fig. 5A and Fig. S5B). However, inspection of the ECM cultures revealed a significantly lower density of cells in cultures with no FGF, or with both FGF2 and BGJ398, than in cultures with FGF2 (Fig. S5A), which was consistent with the role of FGF2 in fibroblast proliferation and survival (Fig. 3A,B). When the amount of collagen detected in ECM cultures was normalized to the cell number, FGF2-treated cultures displayed significantly less collagen than cultures with no FGF or with FGF2 and BGJ398 (Fig. 5B), which was in concordance with decreased expression of fibrillar collagen genes in response to FGF2 detected by qPCR (Fig. 4D).

Analysis of glycosaminoglycans (GAGs) in the fibroblast ECM cultures by Alcian Blue staining revealed significant upregulation of GAGs in FGF2-treated cultures in comparison with mock- or FGF2 and BGJ398-treated cultures (Fig. 5C, Fig. S5C). The amount of GAGs in serum- and serum with BGJ398-treated cultures was underestimated using this method. The bound dye inefficiently eluted from the complex ECM formed in serum- and serum with BGJ398-treated cultures.

Immunofluorescent staining for collagen I, collagen IV and fibronectin detected the presence of these proteins in fibroblast-derived matrices and showed differences in protein amount and organization pattern (Fig. 5D). Overall, the matrices from serum-supplied cultures contained more collagen I, collagen IV and fibronectin, and their staining patterns revealed more complex ECM meshwork than the matrices from serum-low cultures. The matrices from serum-low cultures showed low signal for collagen IV and the staining pattern was more focally organized in FGF2-treated matrices. Moreover, matrices from FGF2-treated cultures displayed higher signal for fibronectin and a lower amount of collagen I than matrices from cultures with no FGF.

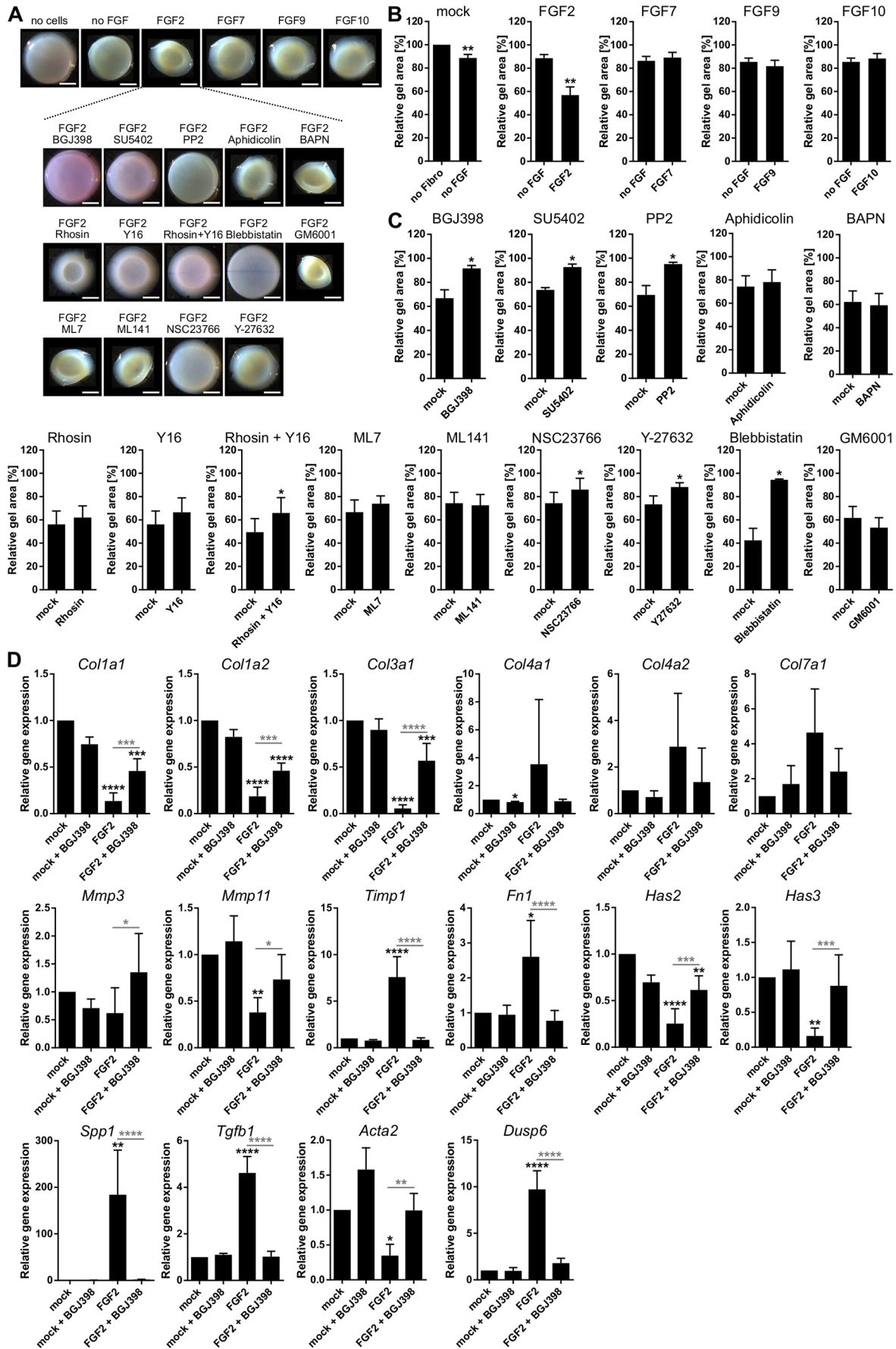


Fig. 4. See next page for legend.

Fig. 4. FGF2 regulates ECM organization and synthesis. (A-C) Collagen contraction assay. Representative photographs of collagen gels (A), treated with FGF ligands or FGF2 with inhibitors as indicated. Scale bars: 5 mm. (B,C) Quantification of collagen gel contraction in response to FGF ligands (B) or FGF2 and inhibitors as indicated (C). Data are mean+s.d., $n=5-11$. * $P<0.05$; ** $P<0.01$ (Student's *t*-test). (D) FGF2 regulates expression of ECM genes. The plots show relative expression of candidate genes on day 7 of FGF2 treatment as mean+s.d., $n=3$. Black asterisks indicate significant change compared with mock (no FGF and no inhibitor). Gray asterisks indicate significant change of a sample treated with FGFR inhibitor (BGJ398) compared with its respective control without inhibitor (as indicated by the gray lines). * $P<0.05$; ** $P<0.01$; *** $P<0.001$; **** $P<0.0001$ (one-way ANOVA).

Scanning electron microscopy revealed structural differences in matrices produced by mammary fibroblasts. The most complex and highly organized matrix was produced by fibroblasts cultured with serum (Fig. 5E). Fibroblasts cultured in serum-low medium without FGF supplementation produced a less-organized matrix of rather thin fibers and material of less distinctive structure. The matrix produced by fibroblasts treated with FGF2 contained thick fibers with small bulbous structures (Fig. 5E). This phenotype reflected the sum effect of FGF2-induced ECM gene expression changes and traction force-mediated remodeling.

FGF signaling in fibroblasts enhances fibroblast-induced branching of mammary epithelium

Stromal fibroblasts are important regulators of mammary epithelial morphogenesis (Hammer et al., 2017; Koledova et al., 2016; Morsing et al., 2016; Peuhu et al., 2017). Therefore, we investigated the role of FGF signaling in fibroblasts in epithelial branching morphogenesis using 3D cultures of mammary organoids alone, and co-cultures of organoids with fibroblasts. In agreement with published data, we observed that organoids did not branch when cultured alone in basal medium without the addition of any growth factor. However, when co-cultured with fibroblasts, organoids formed branched structures (Koledova et al., 2016). Importantly, inhibition of paracrine and autocrine FGF signaling by protamine sulfate, an antagonist of FGF co-receptor heparan sulfate (Wolzt et al., 1995), abrogated fibroblast-induced branching (Fig. 6A-C), suggesting that FGF signaling is involved in fibroblast-induced branching.

Therefore, we investigated whether FGF ligands are increased in organoid-fibroblast co-cultures. Using a growth factor array, we detected low levels of FGF2 protein in organoid cultures, and increased amounts of FGF2 in fibroblast cultures and in organoid-fibroblast co-cultures (Fig. 6D). Other differentially abundant growth factors were amphiregulin (AREG) and hepatocyte growth factor (HGF). In agreement with the reports on production of AREG by mammary epithelium (Ciarloni et al., 2007; Sternlicht et al., 2005), we found high abundance of AREG in organoid cultures, barely detected it in fibroblast cultures, and found moderate amounts of AREG in organoid-fibroblast co-cultures (Fig. 6D). On the other hand, HGF, a potent inducer of mammary epithelial branching morphogenesis (Garner et al., 2011; Gastaldi et al., 2013; Pavlovich et al., 2010), was highly produced in fibroblast cultures, and its production was even higher in co-cultures (Fig. 6D). We also detected the presence of TGF β , a negative regulator of mammary epithelial branching morphogenesis (Silberstein and Daniel, 1987), in all 3D (co-)cultures. qPCR analysis of the 3D (co-)cultures confirmed organoid-specific expression of *Areg* and fibroblast-specific or enriched expression of *Fgf2* and *Hgf*, and revealed increased expression of positive (*Fgf2* and *Hgf*) as well as negative

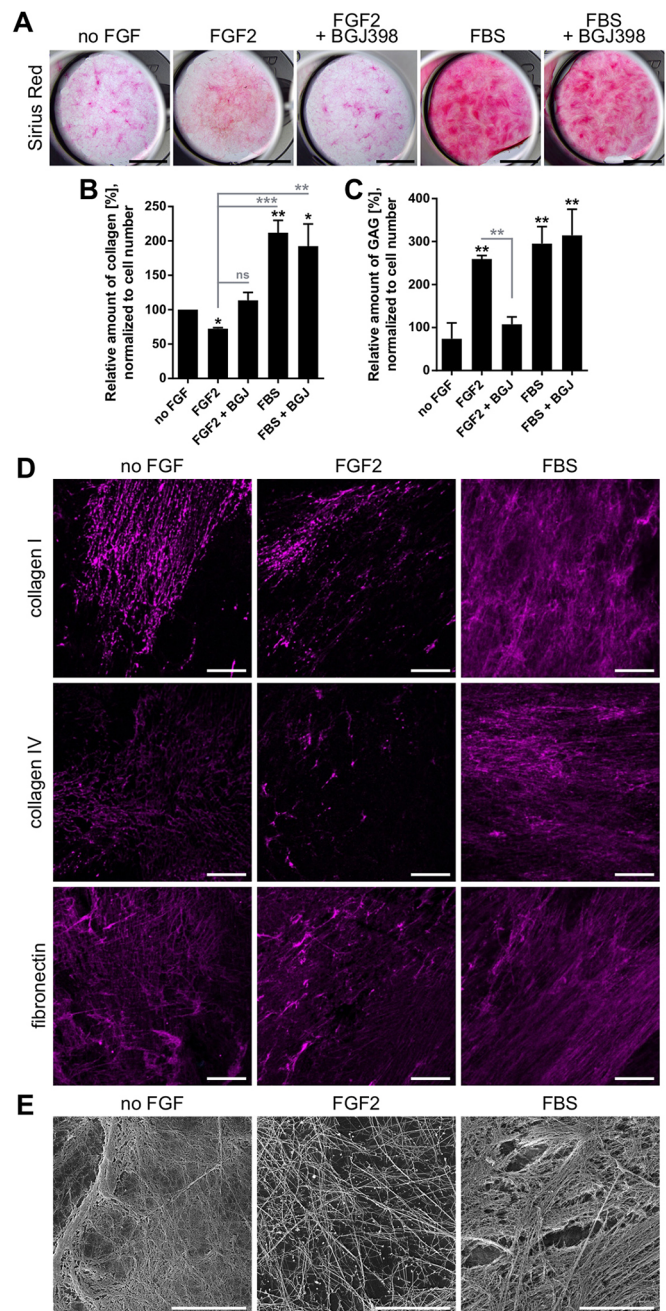


Fig. 5. FGF2 regulates ECM production. (A-C) Detection of collagen and glycosaminoglycan production. Photographs of Sirius Red-stained cell cultures (A). Scale bars: 5 mm. (B,C) Quantification of collagen (B) and glycosaminoglycans (GAG) (C). The graphs show the relative amount of collagen or GAG under different treatments in comparison with culture with no FGF, normalized to cell number, as mean+s.d.; $n=2-4$. Black asterisks indicate significant change compared with no FGF. Gray asterisks indicate significant change compared with FGF2 (as indicated by the gray lines). * $P<0.05$; ** $P<0.01$; *** $P<0.001$ (one-way ANOVA). ns, not significant. (D) Immunofluorescent staining of cell-derived matrices for collagen I, collagen IV and fibronectin. Scale bars: 20 μ m. (E) Representative images from scanning electron microscopy of decellularized cell-derived matrices. Scale bars: 10 μ m.

(*Tgfb1*) regulators of epithelial branching in co-cultures (Fig. 6E), suggesting that 3D co-cultures provide a complex microenvironment of epithelial-stromal paracrine interactions.

Next, we analyzed whether stimulation of fibroblasts with FGF2 increases epithelial branching. Because FGF2 is a potent yet

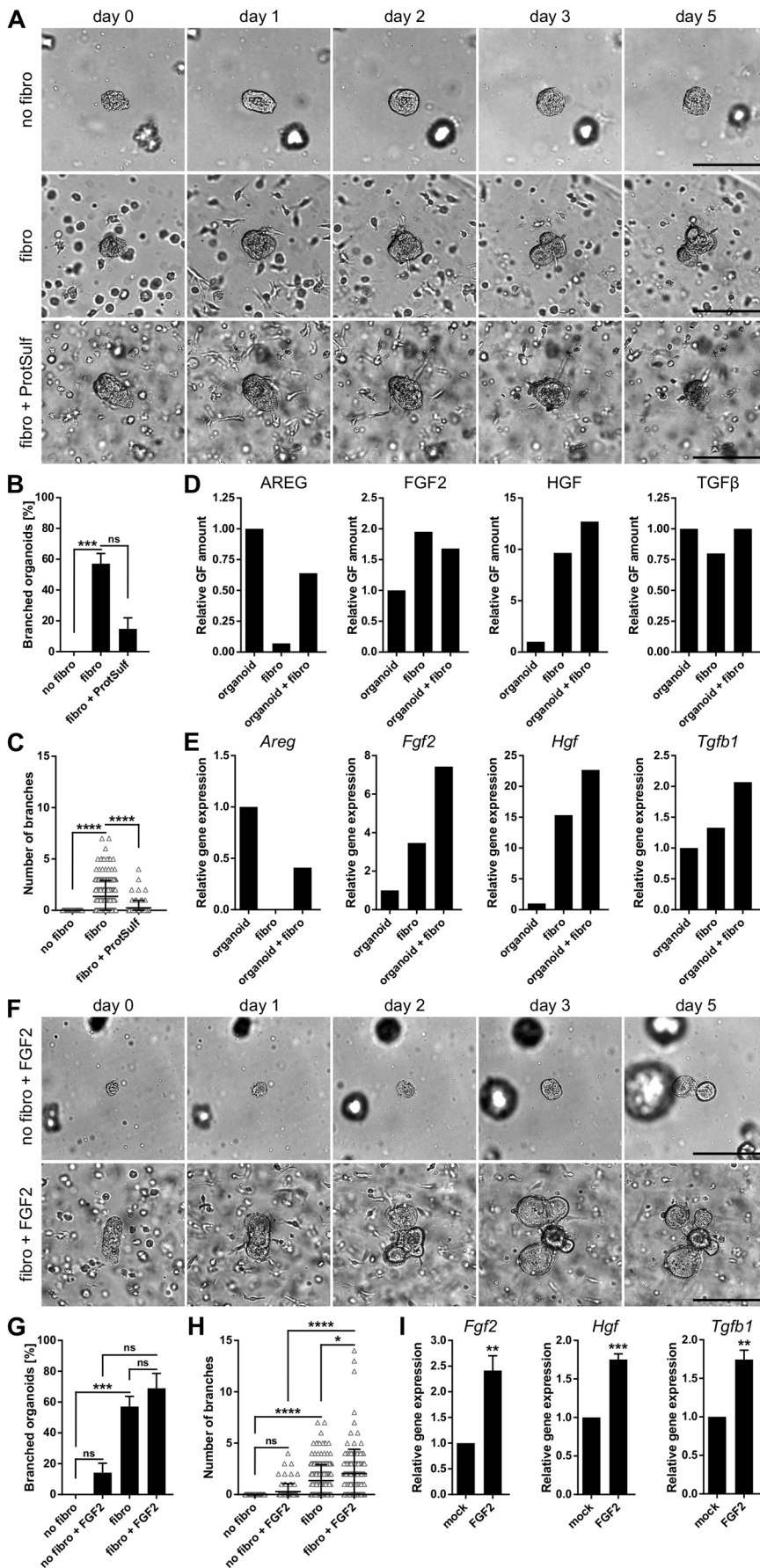


Fig. 6. FGF signaling in mammary fibroblasts enhances fibroblast-induced branching of mammary epithelium. (A-C) Analysis of mammary epithelial organoid branching in response to fibroblasts and protamine sulfate (ProtSulf). 3D cultures of organoids (no fibro) and co-cultures of organoids and fibroblasts (fibro) were treated with ProtSulf as indicated and imaged for 5 days using time-lapse microscopy. Representative snapshots from time-lapse microscopy (A). Scale bars: 100 μ m. Quantification of epithelial organoid branching (B,C). The plots show percentage of branched organoids (B) and the number of branches per organoid (C) (each triangle indicates one organoid; $n=4-10$; 66-238 organoids). Data are mean+s.d. *** $P<0.001$; **** $P<0.0001$ (Kruskal–Wallis test). (D) Growth factor array analysis of 3D cultures of organoids, fibroblasts and 3D co-cultures of organoids with fibroblasts. The plot shows relative signal for growth factors (GF); $n=1$. (E) qPCR analysis of growth factor gene expression in 3D (co-)cultures; $n=1$. (F-H) Analysis of mammary epithelial organoid branching in response to FGF2 and fibroblasts using time-lapse microscopy over 5 days. Representative images (F). Scale bars: 100 μ m. Quantification of epithelial organoid branching (G,H). The plots show percentage of branched organoids (G) and the number of branches per organoid (H) (each triangle indicates one organoid; $n=5-10$; 66-238 organoids). Data are mean+s.d. * $P<0.05$; *** $P<0.001$; **** $P<0.0001$ (Kruskal–Wallis test). (I) qPCR analysis of candidate growth factor gene expression in 3D co-cultures treated with no FGF (mock) or FGF2. Data are mean+s.d., $n=3$. ** $P<0.01$; *** $P<0.001$ (Student's t -test). ns, not significant.

dose-dependent inducer of epithelial branching on its own, we used a low concentration of FGF2 (1 nM) that induced branching in only 14% of organoids in fibroblast-free cultures. In co-cultures with fibroblasts, 1 nM FGF2 increased the frequency of mammary organoid branching from 57% (no FGF2) to 69% (with FGF2; Fig. 6F,G), though this change was not statistically significant. However, the number of branches per organoid was significantly increased in co-cultures treated with FGF2 (Fig. 6H) and the organoid branches were more prominently developed in co-cultures treated with FGF2 than in co-cultures without FGF treatment (Fig. 6A,F). In co-cultures treated with FGF2, we detected increased expression of *Fgf2*, *Hgf* and *Tgfb1* in comparison with co-cultures not treated with FGF2 (Fig. 6I), suggesting that FGF2 increased production of regulators of epithelial branching. Moreover, we found that FGF2 treatment induced *Fgf2* expression in fibroblasts (Fig. S6), suggesting a potential autocrine FGF2 signaling loop in fibroblasts. Yet, we could not exclude a direct pro-branching effect of the low dose FGF2 on epithelium.

Therefore, we tested the capacity of FGF9 to induce mammary epithelial branching in 3D co-cultures. FGF9 is expressed in pubertal mammary gland (Zhang et al., 2014b) and showed activity in mammary fibroblasts (Fig. 2A-C, and Fig. 3A-E), but it did not induce any epithelial branching in organoid-only cultures (Fig. 7A, B and Fig. S7). However, in co-cultures with fibroblasts, FGF9 increased the frequency of mammary organoid branching (from 70% with no FGF9 to 85% with FGF9; Fig. 7A,B) and, moreover, significantly increased the number of branches per organoid (Fig. 7C). These results suggested that stimulation of fibroblasts with FGF9 promotes their abilities to induce epithelial branching. To address an alternative possibility that FGF9 could synergize with fibroblast-derived growth factors to directly stimulate epithelial branching, we tested the ability of FGF9 to induce branching in fibroblast-free mammary organoid cultures, in which we modeled the effect of fibroblast-derived growth factors by low FGF2 concentration (1 nM). We found that FGF9 did not increase organoid branching in the presence of 1 nM FGF2 (Fig. S7).

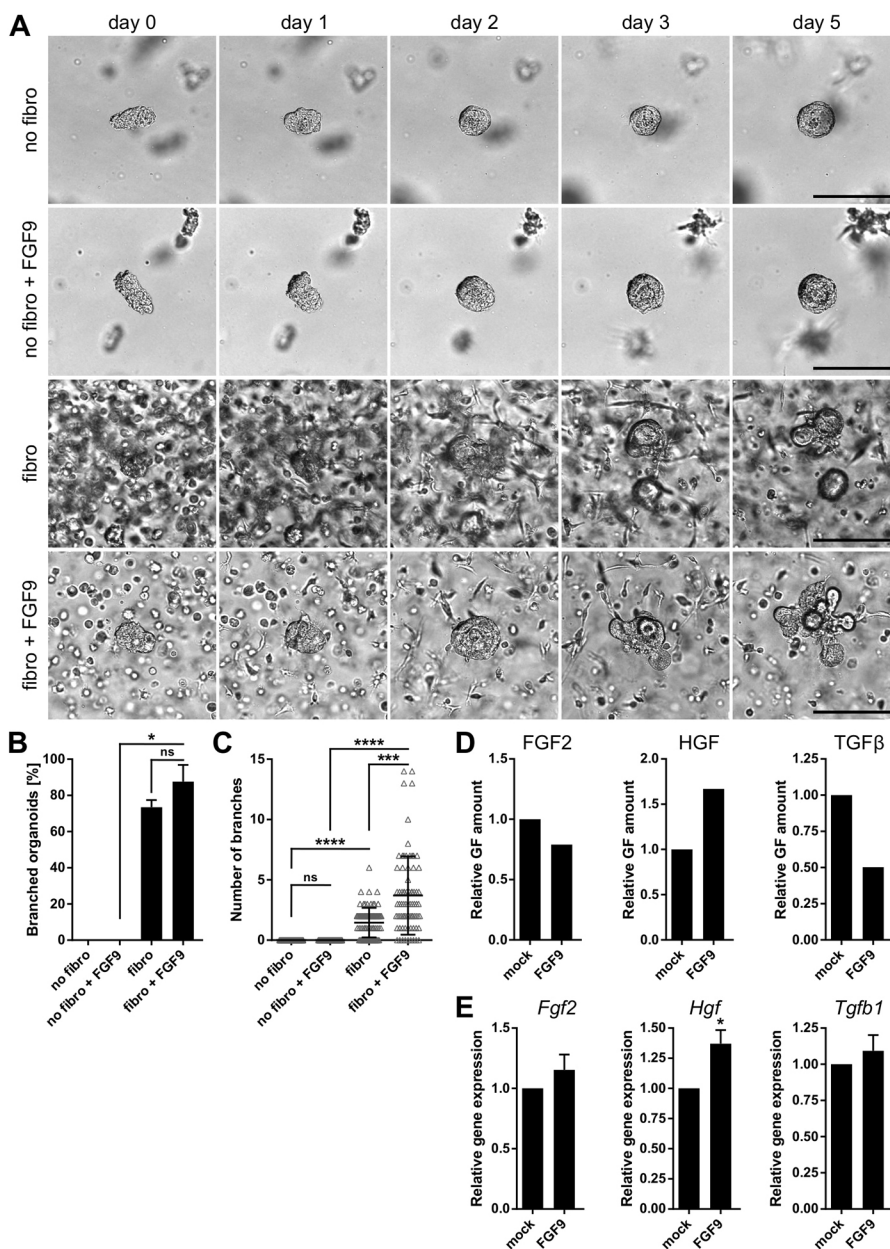


Fig. 7. FGF9 signaling in mammary fibroblasts enhances fibroblast-induced branching of mammary epithelium. (A-C) Analysis of mammary epithelial organoid branching in response to fibroblasts and FGF9. 3D cultures of organoids (no fibro) and co-cultures of organoids and fibroblasts (fibro) were treated with no FGF or with FGF9 and imaged for 5 days using time-lapse microscopy. Representative images from time-lapse microscopy (A). Scale bars: 100 μ m. Quantification of epithelial organoid branching (B,C). The plots show percentage of branched organoids (B) and the number of branches per organoid (C) (each triangle indicates one organoid; $n=4$; 74-80 organoids). Data are mean+s.d. * $P<0.05$; *** $P<0.001$; **** $P<0.0001$ (Kruskal-Wallis test). (D) Growth factor array analysis of 3D co-cultures of organoids with fibroblasts, treated with no FGF or FGF9. The plots show relative growth factor (GF) signal; $n=1$. (E) qPCR analysis of candidate growth factor gene expression in 3D co-cultures treated with no FGF (mock) or FGF9. Data are mean+s.d., $n=3$. * $P<0.05$ (Student's *t*-test). ns, not significant.

Therefore, the epithelial branching-stimulating effect of FGF9 in co-cultures was most likely mediated by fibroblasts. Analysis of growth factor production in co-cultures using a growth factor array revealed an increased amount of HGF and a decreased amount of TGF β in FGF9-treated co-cultures, compared with untreated co-cultures (Fig. 7D). qPCR analysis of the co-cultures confirmed increased expression of *Hgf* and showed no significant change in *Fgf2* and *Tgfb1* expression in response to FGF9 (Fig. 7E). Taken together, our results suggest that FGF2 and FGF9 regulate expression of positive and negative regulators of mammary epithelial branching, including FGF2, HGF and TGF β , in fibroblasts, and that the interplay of these regulators influences epithelial branch formation and patterning.

Knockdown of *Fgfr1* and *Fgfr2* in mammary fibroblasts reduces fibroblast-induced branching of mammary epithelium

To further test whether FGFR signaling in fibroblasts regulates branching of mammary epithelium, we knocked down *Fgfr1* and *Fgfr2* in mammary fibroblasts using two different small interfering RNAs (siRNAs) for both genes, and we tested the ability of *Fgfr* knockdown fibroblasts to induce epithelial branching in 3D co-cultures. The efficiency of *Fgfr1* knockdown, measured using qPCR for the *Fgfr1c* isoform that is expressed in mammary fibroblasts (Fig. 1A), was 72% and 90% using *Fgfr1* siRNA#1 and *Fgfr1* siRNA#2, respectively (Fig. 8A). The efficiency of *Fgfr2* knockdown was 59% and 30% by *Fgfr2* siRNA#1 and *Fgfr2* siRNA#2, respectively, as measured using qPCR for the *Fgfr2c* isoform (Fig. 8A).

In 3D co-culture experiments, when no FGF was added to the medium, knockdown of *Fgfr1* and *Fgfr2* in mammary fibroblasts significantly decreased branching of mammary epithelium by 43% to 49% (Fig. 8B). In co-cultures stimulated by 1 nM FGF2, *Fgfr1* or *Fgfr2* knockdown in fibroblasts reduced branching of mammary epithelium by 41% to 64%. (Fig. 8C). These results unambiguously demonstrate the role of FGFR signaling in stromal fibroblasts in the

regulation of mammary epithelial branching in 3D organotypic co-cultures.

DISCUSSION

Fibroblasts are important regulators of mammary epithelial morphogenesis (Hammer et al., 2017; Koledova et al., 2016; Kuperwasser et al., 2004; Morsing et al., 2016; Peuhu et al., 2017; Zhang et al., 2002), but the regulation of fibroblast function is incompletely understood. In this study, we identified functional components of FGF signaling in mammary fibroblasts and their roles in regulation of multiple biological functions, including fibroblast proliferation, migration, ECM production and remodeling, and interactions with mammary epithelium during mammary epithelial branching morphogenesis.

We found expression of FGFR1 and FGFR2 in the mammary fibroblasts, both in their IIIc variants. This is consistent with the distinct spatial expression patterns of the FGFR splice variants, with the IIIc variants preferentially found in the mesenchyme and the IIIb variants more common in epithelia (Kettunen et al., 1998; Orr-Urtreger et al., 1993; Rice et al., 2003). Moreover, in agreement with the FGF ligand specificity of the IIIc variants of FGFR1 and FGFR2 (Ornitz and Itoh, 2015), we detected functional response (such as proliferation and 2D migration) of mammary fibroblasts to FGF2 and FGF9, but no functional response was elicited by FGF7 or FGF10, which activate specifically FGFR IIIb variants. The lack of functional outcome in response to FGF7 and FGF10 corresponded to only weak and transient activation of ERK1/2, whereas FGF2 and FGF9 elicited strong and sustained ERK1/2 activation. These observations are in agreement with a previous study that showed ERK1/2 signaling dynamics is the key determinant of cellular response to FGF signaling (Zhu et al., 2010). Moreover, differences in AKT signaling engagement in response to FGF2 and FGF9 that we observed, and/or distinct FGFR signaling kinetics (Francavilla et al., 2013), could underlie the distinct capability of FGF2 to promote fibroblast migration in 3D ECM and force-mediated collagen remodeling.

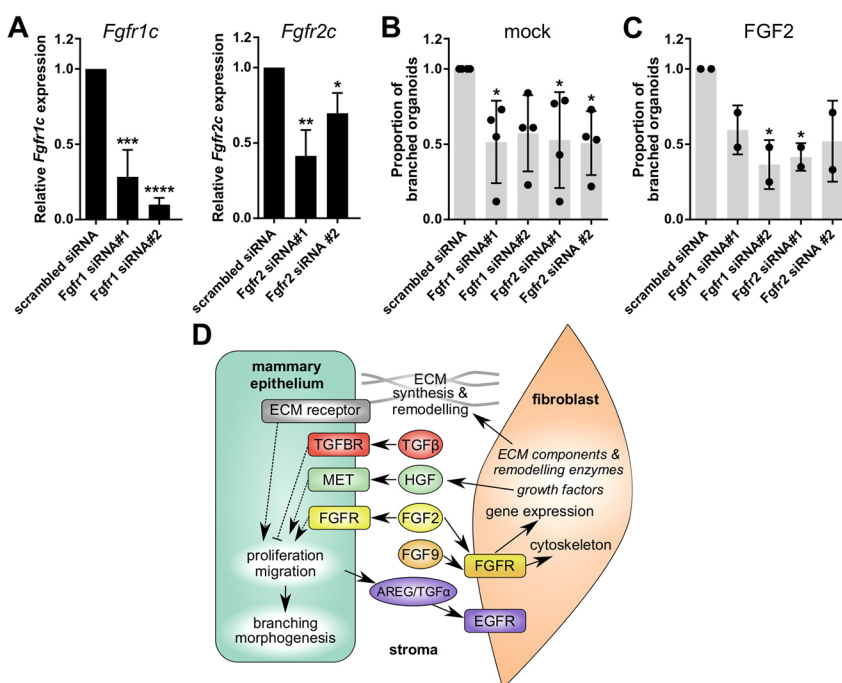


Fig. 8. Knockdown of *Fgfr1* or *Fgfr2* in mammary fibroblasts reduces fibroblast-induced branching of mammary epithelium. (A) qPCR analysis of *Fgfr1c* and *Fgfr2c* mRNA levels 48 h after siRNA transfection. Data are mean \pm s.d., $n=3$. * $P<0.05$; ** $P<0.01$; *** $P<0.001$; **** $P<0.0001$ (one-way ANOVA). (B,C) Analysis of mammary epithelial organoid branching in response to *Fgfr1* or *Fgfr2* knockdown fibroblasts. 3D co-cultures of organoids with siRNA-transfected fibroblasts were treated with no FGF (mock, B) or with FGF2 (C) and imaged for 5 days using time-lapse microscopy. Quantification shows proportion of branched organoids as mean \pm s.d.; $n=4$ (B; $N=80$ organoids per condition) or $n=2$ (C; $N=40$ organoids per condition). * $P<0.05$ (one-way ANOVA). The points show individual values from independent biological replicates. (D) Schematic of the role of FGF signaling in fibroblasts in regulation of mammary epithelial branching morphogenesis.

Our investigation of the mechanism of FGF2-induced fibroblast migration in 3D ECM by inhibition of candidate molecules revealed a requirement for Rho GTPases (RAC1, Cdc42), which regulate actin dynamics, and MLCK, which phosphorylates myosin regulatory light chain 2 (MLC2) to regulate activity and assembly of myosin II filaments (Sit and Manser, 2011). Intriguingly, inhibition of ROCK, which also phosphorylates MLC2, enhanced fibroblast migration. This could be, at least in part, explained by MLCK and ROCK acting on distinct myosin II pools (Totsukawa et al., 2004). Inhibition of myosin II using blebbistatin induced massive amoeboid-like migration of fibroblasts, which is consistent with a role for low contractility in this switch in migration mode (Liu et al., 2015).

ECM signals, including ECM composition, stiffness and topology, regulate mammary epithelial cell adhesion, migration, proliferation, apoptosis, survival and differentiation, and thereby determine mammary epithelial morphogenesis (Bonnans et al., 2014; Schedin and Keely, 2011). For example, patterning of collagen fibers in the mammary gland stroma regulates the orientation of terminal end buds during branching morphogenesis (Brownfield et al., 2013). Recent publications have reported the important role of fibroblasts in regulation of ECM composition, abundance and organization, and thereby in regulation of mammary epithelial branching morphogenesis (Feinberg et al., 2018; Hammer et al., 2017; Koledova et al., 2016; Morsing et al., 2016; Peuhu et al., 2017). We found that FGF signaling in fibroblasts regulates expression of several ECM genes, including collagens. FGF2 downregulated expression of genes for fibrillar collagens I and III, the major structural proteins of connective tissues, including mammary gland ECM. FGF2 was also found to regulate expression of several genes involved in the regulation of collagen abundance and organization, including *Mmp11* and *Timp1*, a regulator of MMPs. Moreover, FGF2 induced expression of *Tgfb1*, a growth factor involved in the regulation of ECM production and remodeling during development, as well as in cancer progression (Moses and Barcellos-Hoff, 2011). Furthermore, Alcian Blue staining revealed upregulation of GAGs in the fibroblast-derived ECM due to FGF2, which corresponded to upregulation (though statistically insignificant) of the HSPG *Sdc1*. Because HSPGs bind FGFs and act as FGF signaling co-receptors (Bernfield et al., 1999; Mundhenke et al., 2002), such regulation could form a positive FGF signaling loop in mammary fibroblasts.

Mammary fibroblasts reorganize collagen fibers by exerting traction forces during cell adhesion and migration in 3D ECM (Peuhu et al., 2017). We found that FGF signaling promotes traction force-mediated collagen remodeling. Activity of MMPs or LOX, the proteins involved in collagen remodeling by proteolytic cleavage or crosslinking, respectively (Bonnans et al., 2014), did not contribute to FGF2-induced collagen remodeling in a collagen contraction assay. Moreover, although FGF2 also regulates fibroblast proliferation, differences in cell proliferation in response to FGF ligands were unlikely to account for the distinctive FGF2-induced collagen gel contraction, as inhibition of cell proliferation did not abrogate it. This is consistent with the reports that fibroblasts do not proliferate in floating collagen gels (Grinnell, 2000).

Our findings are consistent with the well-known role of FGF signaling in other stromal cell types, such as skin fibroblasts, in the regulation of cell proliferation, migration, and ECM production and organization in development, wound healing and tissue regeneration, including the anti-scar effects of FGF2 (Maddaluno et al., 2017; Shi et al., 2013). These functions can be regulated by FGF signaling both directly (Ko and Kay, 2005) as well as

indirectly, through FGF-regulated growth factors, such as TGF β (Shi et al., 2013) or HGF (Suga et al., 2009) that mediate the FGF effect. Because we found that FGF signaling in mammary fibroblasts regulates expression of TGF β and HGF, the phenotypes that we observed are most likely a net result of both direct and indirect regulation by FGF signaling.

Furthermore, fibroblasts orchestrate mammary epithelial morphogenesis using paracrine signaling (Koledova et al., 2016; Zhang et al., 2002). In this study, we showed that fibroblasts produce several regulators of mammary epithelial branching, including FGF2, HGF and TGF β , and that co-culture of fibroblasts with mammary epithelial organoids induced organoid branching. Moreover, we showed that stimulation of FGF signaling in fibroblasts by FGF2 or FGF9 increased epithelial branching frequency. FGF2 is a potent inducer of mammary epithelial branching (Ewald et al., 2008) in a dose-dependent manner (Zhang et al., 2014a). In the co-cultures treated with FGF2, the epithelium was also unavoidably exposed to FGF2. But the dose that we used to stimulate fibroblasts was by itself inefficient in induction of pronounced epithelial branching. In the co-cultures, low dose FGF2 increased the frequency of epithelial organoid branching and significantly increased the number of branches formed. We also detected increased expression of paracrine regulators of mammary epithelial branching in response to FGF2, including the positive regulators *Fgf2* (Ewald et al., 2008; Sternlicht et al., 2005) and *Hgf* (Garner et al., 2011; Gastaldi et al., 2013; Pavlovich et al., 2010), and the negative regulator *Tgfb1* (Silberstein and Daniel, 1987). Therefore, we conclude that the epithelial branching in FGF2-treated co-cultures was predominantly caused by fibroblast-mediated signaling and that branching frequency and patterning were determined by the net effect of positive and negative regulatory signals, their spatial distribution and temporal fluctuations.

Further tests using FGF9 provided even stronger evidence for the role of FGF signaling in fibroblasts in fibroblast-induced epithelial branching. FGF9 did not induce mammary epithelial organoid branching at all in fibroblast-free cultures; in the absence of fibroblasts, FGF9 had a negative effect on FGF2-induced epithelial branching. This unexpected effect could stem from competition for receptors, such as FGFRs or HSPGs (Forsten-Williams et al., 2008; Yamagishi and Okamoto, 2010), and modulation of ERK1/2 signaling dynamics, the central determinant of mammary epithelial morphogenesis (Fata et al., 2007). Importantly, in organoid-fibroblast co-cultures, FGF9 increased the frequency of fibroblast-induced epithelial branching and significantly increased the number of branches per organoid. This effect was at least in part mediated by an FGF9-induced increase in HGF.

The ultimate evidence for the role of FGF signaling in fibroblasts in mammary epithelial branching came from *Fgfr1* and *Fgfr2* knockdown experiments, which showed that knockdown of *Fgfr1* or *Fgfr2* in mammary fibroblasts significantly reduced mammary epithelial branching in 3D co-cultures. The fact that *Fgfr1* or *Fgfr2* knockdown in fibroblasts did not completely abrogate epithelial branching is probably caused by the knockdown efficiency of 30-90%, but it could also indicate presence of other, FGFR-independent, mechanism(s) of fibroblast-induced branching.

Together, we presented evidence for a role of FGF signaling in mammary fibroblasts in mammary epithelial branching morphogenesis by regulation of ECM remodeling and paracrine signaling (Fig. 8D). Our results show that FGF signaling in mammary fibroblasts regulates production of ECM structural proteins and remodeling enzymes, as well as contributes to force-induced ECM remodeling, either directly, or indirectly through

regulation of growth factors that regulate these fibroblast functions. ECM composition, stiffness and organization is, in turn, sensed by the epithelium and affects epithelial morphogenesis. Moreover, FGF signaling in fibroblasts regulates the production of paracrine signals that regulate epithelial branching, including FGF2, HGF and TGF β . In the mammary gland, and analogously in the 3D co-culture, the communication between stromal and epithelial cells is bidirectional, i.e. epithelial cells also signal to stromal cells. AREG is one of the known epithelium-derived signals for stromal cells that is required for epithelial branching (Ciarloni et al., 2007; Sternlicht et al., 2005). In our experiments, we detected AREG expression by organoids and moderate levels of AREG were present in the co-cultures. However, it remains to be determined whether and how AREG signaling is integrated with FGF signaling in mammary fibroblasts.

Our findings from 2D and 3D cultures lay the ground for further studies on the role of FGF signaling in mammary fibroblasts in the context of the whole mammary gland using mouse models, which would provide a physiological, more complex microenvironment and allow for the analysis of long-term effects of FGF signaling modulation in fibroblasts. Moreover, fibroblasts are a key component of breast cancer stroma and a determinant of breast cancer progression (Ahn et al., 2012; Cid et al., 2018; Kalluri and Zeisberg, 2006). Their protumorigenic effects include production of paracrine proliferative and proinvasive signals to cancer cells (Bernard et al., 2018; Orimo et al., 2005), ECM remodeling to enable invasion of cancer cells (Gaggioli et al., 2007) and enabling immune evasion (Chakravarthy et al., 2018). Because increased expression of FGF ligands, including FGF1, FGF2 and FGF7, was found in breast cancer stroma in comparison with normal breast stroma (Finak et al., 2008; Relf et al., 1997), it is relevant to investigate the role of FGF signaling in breast cancer-associated fibroblasts.

MATERIALS AND METHODS

Mice

This study used female ICR mice, obtained from the Laboratory Animal Breeding and Experimental Facility of the Faculty of Medicine, Masaryk University, the Czech Republic. Experiments involving animals were approved by the Ministry of Agriculture of the Czech Republic, supervised by the Expert Committee for Laboratory Animal Welfare at the Faculty of Medicine, Masaryk University, and performed by certified individuals (Z.K., J.S.). The study was carried out in accordance with the principles of the Basel Declaration.

Primary mammary organoid and fibroblast isolation and culture

Primary mammary fibroblasts and organoids were isolated from 6-8-week-old female ICR mice as previously described (Koledova, 2017). Briefly, the mice were euthanized by cervical dislocation. The mammary glands were removed, mechanically disintegrated and partially digested in a solution of collagenase and trypsin [2 mg/ml collagenase A, 2 mg/ml trypsin, 5 μ g/ml insulin, 50 μ g/ml gentamicin (all Sigma-Aldrich/Merck), 5% fetal bovine serum (FBS; Hyclone/GE Healthcare) in DMEM/F12 (Thermo Fisher Scientific)] for 30 min at 37°C. The resulting tissue suspension was treated with DNase (20 U/ml; Merck) and exposed to five rounds of differential centrifugation (450 g), which resulted in separation of epithelial (organoid) and stromal fractions. The organoids were resuspended in basal organoid medium [1 \times ITS (10 μ g/ml insulin, 5.5 μ g/ml transferrin, 6.7 ng/ml sodium selenite), 100 U/ml of penicillin and 100 μ g/ml of streptomycin in DMEM/F12] and kept on ice until used for co-culture experiments. The cells from the stromal fraction were pelleted by centrifugation (600 g), suspended in fibroblast cultivation medium (10% FBS, 1 \times ITS, 100 U/ml of penicillin and 100 μ g/ml of streptomycin in DMEM) and incubated on cell culture dishes at 37°C in 5% CO₂ for 30 min. Next, selection by differential attachment was performed to remove non-fibroblast cells: After the 30 min

incubation, unattached cells were washed away, the cell culture dishes were washed with PBS and fresh fibroblast medium was provided. The cells were cultured until ~80% confluence. During the first cell subculture by trypsinization, a second round of selection by differential attachment was performed, when the cells were allowed to attach only for 15 min at 37°C and 5% CO₂. The cells were expanded and used for the experiments until passage 5.

Immunohistochemistry of mammary gland

Mammary glands from 6-week-old female ICR mice were fixed with neutral buffered formalin overnight at room temperature (RT). The next day, the tissue was rinsed in tap water, dehydrated in an ethanol series of ascending concentration up to 100%, and embedded in paraffin. Paraffin sections were cut (5 μ m thickness), deparaffinized using xylene and rehydrated. Antigens were retrieved using Tris-EDTA buffer (pH 9; Dako) and endogenous peroxidase activity was blocked using 3% hydrogen peroxide. The sections were blocked in PBS with 10% FBS and incubated with primary antibody (Table S1) for 1 h at RT. After washing, sections were incubated with secondary antibody (EnVision+ Dual Link System-HRP; K4061; Dako) for 30 min at RT. After washing, bound secondary antibody was detected using Liquid DAB+ Substrate Chromogen System (Dako). The nuclei were stained with Mayer's Hematoxylin, dehydrated and mounted in Pertex (Histolab Products). The samples were photographed using a Leica DM5000 microscope equipped with a Leica DFC480 camera.

Immunofluorescence staining of fibroblasts

Fibroblasts were cultured directly on coverslips, or in a Matrigel (Corning) droplet on coverslips, fixed with neutral buffered formalin, permeabilized with 0.05% Triton X-100 in PBS and blocked with PBS with 10% FBS. Then the cells were incubated with primary antibodies (Table S1) for 2 h at RT or overnight at 4°C. After washing, the cells were incubated with secondary antibodies (Table S1) and Alexa Fluor 488 Phalloidin (Thermo Fisher Scientific). Then the cells were washed, stained with DAPI (1 μ g/ml; Merck) for 10 min and mounted in Mowiol (Merck). The cells were photographed using an Eclipse Ti microscope (Nikon) or a LSM 800 (Zeiss).

Western blotting

Fibroblast cultures were washed twice with ice-cold PBS and subsequently lysed in RIPA buffer [150 mM NaCl, 1.0% NP-40, 0.5% sodium deoxycholate, 0.1% SDS, 50 mM Tris (pH 8.0)] and supplied with proteinase and phosphatase inhibitors (10 mM β -glycerophosphate, 5 mM NaF, 1 mM Na₃VO₄, 1 mM dithiothreitol, 0.5 mM phenylmethanesulphonyl fluoride, 2 μ g/ml aprotinin, 10 μ g/ml leupeptin; all Merck). Protein lysates were homogenized by vortexing, cleared by centrifugation (12,000 g), and protein concentration was measured using the Bradford reagent. Denatured, reduced samples were resolved on 10% SDS-PAGE gels and blotted onto PVDF membranes (Merck). For FGFR detection, wet transfer was used (in 190 mM glycine, 25 mM Tris, 20% methanol). For detection of ERK, AKT, including their phosphorylated variants, and β -actin, semi-dry transfer was used [in 50 mM Tris, 40 mM glycine, 0.037% (v/v) SDS, 20% methanol]. Membranes were blocked with 5% non-fat milk in PBS with 0.05% Tween-20 (Merck; blocking buffer) and incubated with primary antibodies (Table S1) diluted in blocking buffer overnight at 4°C. After washing in PBS with 0.05% Tween-20, the membranes were incubated with horseradish peroxidase-conjugated secondary antibodies (Table S1) for 1 h at RT. Signal was developed using a chemiluminescence substrate [100 mM Tris-HCl (pH 8.5), 0.2 mM coumaric acid, 1.25 mM luminol, 0.01% H₂O₂; all Merck] and exposed on X-ray films (Agfa), which were then scanned and band density was analyzed in ImageJ (National Institutes of Health) using the western blot densitometry analysis macro tool for ImageJ 1.x (<https://github.com/cernekj/WBGelDensitometryTool>). Phosphorylated and total proteins and β -actin were analyzed on a single blot.

MTT and resazurin assays

For the proliferation assay in 2D, 5 \times 10³ or 7 \times 10³ cells per well were seeded in 96-well plates in fibroblast cultivation medium. The next day the plates were carefully washed three times with PBS and supplied with serum-low medium (0.2% FBS, 0.1 \times ITS, 100 U/ml of penicillin, 100 μ g/ml of

streptomycin in DMEM) and incubated for 24 h at 37°C, 5% CO₂. The next day FGF ligands (to 5 nM) and heparin (to 2 µg/ml; Merck) were added. All treatments were carried out in intraexperimental triplicates. The cells were incubated with FGF ligands for 24 h. Then MTT (Merck) was added to the plate to the final concentration 0.45 mg/ml and the plates were incubated for 5 h at 37°C, 5% CO₂. Then, medium was aspirated and formazan crystals were dissolved in 10% SDS, 0.01 M HCl. MTT absorbance (at 570 nm) was measured using Synergy HTX microplate reader (Bio-Tek).

For FGFR inhibition assay, 5×10^3 or 7×10^3 cells per well were seeded in 96-well plates in fibroblast cultivation medium. The next day, FGFR inhibitors BGJ398 (Selleckchem) and SU5402 (Merck) were added at a range of concentrations (in intraexperimental triplicates) and incubated for 24 or 48 h. Then MTT assay was performed as described above. IC₅₀ values were calculated from normalized data using nonlinear regression in GraphPad Prism.

For the proliferation assay in 3D, 2×10^4 fibroblasts were plated in 3D Matrigel. The gels were incubated for 30 min at 37°C to solidify, then fibroblast starvation medium (1× ITS, 100 U/ml of penicillin, 100 µg/ml of streptomycin in DMEM) was added and the cells were cultured overnight. Next day, the cells were treated with 5 nM FGF2, FGF7, FGF9 or FGF10 in fibroblast starvation medium with heparin (4 µg/ml) and incubated for 24 h. Subsequently, resazurin (Merck) was added to a final concentration of 10 µg/ml and the cells were incubated for 23 h at 37°C, 5% CO₂. Resorufin fluorescence (excitation at 560 nm, emission at 590 nm) was measured using Synergy H4 Hybrid multi-mode microplate reader (Bio-Tek).

Scratch assay

Fibroblasts were seeded in 12-well plate and grown to full confluence in fibroblast cultivation medium. Then the cells were washed three times with PBS and cultured for 24 h in serum-low medium [0.2% heat-inactivated FBS (FBS-HI), 0.1× ITS, 100 U/ml of penicillin and 100 µg/ml of streptomycin in DMEM]. Next day, the scratch was induced using a 200 µl pipette tip, the cells were washed three times with PBS and treated with 5 nM FGF2, FGF7, FGF9, FGF10, or no FGF, in serum-low medium with 2 µg/ml heparin. To test the effect of inhibition of cell proliferation on cell migration, the cells were treated with 10 µg/ml mitomycin C (Merck) for 2 h before scratch introduction, or with 2.93 µM aphidicolin for the whole duration of the assay. The plate was incubated in a humidified atmosphere of 5% CO₂ at 37°C on an Olympus IX81 microscope equipped with a Hamamatsu camera and CellR system for time-lapse imaging. The scratch areas (six non-overlapping areas per well) were photographed every hour for 24 h or until they were closed by migrating cells (when cells from opposite sides of the scratch met) in at least one of the imaged positions. The first occasion of scratch closure was set as the experimental endpoint (typically 11-19 h after scratch induction). The images were exported and analyzed using ImageJ. The first and endpoint image for each position were overlaid, cells that migrated were counted and their migration distance was measured (perpendicular to the scratch median line). The average total migration distance per condition was calculated and compared with the average total migration distance of cells with no FGF treatment.

Transwell migration assay

For the transwell migration assay, 1×10^5 fibroblasts were seeded in the upper chamber of the transwell insert (polycarbonate membrane, 8 µm pore size; Corning) in transwell assay medium [0.1% bovine serum albumin (BSA), 2 µg/ml heparin in DMEM]. In the lower chamber, transwell assay medium with 5 nM FGF2, FGF7, FGF9 or FGF10 was added. The cells were incubated for 10-11 h at 37°C, 5% CO₂. Then the filter side of the upper chamber was wiped with a cotton swab to remove non-migratory cells and the remaining cells on the opposite side of the membrane were fixed with 4% paraformaldehyde for 15 min, washed with distilled water and stained with 0.1% Crystal Violet (Merck) for 15 min. After washing with distilled water, the membranes were cut from the inserts and the number of migrated cells was counted using an Olympus IX81 microscope.

Fibrosphere 3D migration assay

The fibroblasts were aggregated into fibrospheres by overnight culture at high density in fibroblast medium in bacterial dishes as previously

described (Koledova, 2017). The fibrospheres were collected, washed three times with PBS, mixed with Matrigel and plated in 3D domes. The cultures were incubated for 45 min at 37°C, 5% CO₂, then basal fibrosphere medium (1× ITS, 100 U/ml of penicillin and 100 µg/ml of streptomycin in DMEM) was added, supplied with 5 nM FGF ligands and/or inhibitors (Table S2). The cultures were incubated in a humidified atmosphere of 5% CO₂ at 37°C on an Olympus IX81 microscope equipped with a Hamamatsu camera and CellR system for time-lapse imaging. The fibrospheres were photographed every 60 min for 48 h. The images were exported and analyzed using ImageJ. For each fibrosphere, the length of all protrusions was measured radially from the edge of the fibrosphere body to the end of the protrusion.

Analysis of FGF signaling dynamics

Fibroblasts were grown to desired confluence, washed three times with PBS and serum-starved in DMEM with 0.05× ITS, 100 U/ml of penicillin and 100 µg/ml of streptomycin. Next day, the cells were treated with 5 nM FGF ligands in DMEM with 4 µg/ml heparin for 5 to 60 min. After treatment, cells were immediately washed twice with ice-cold PBS and lysed in the RIPA buffer and further processed for western blotting as described above.

Analysis of ECM production

Fibroblasts were cultured to full confluence, then washed three times with PBS and treated with ECM starvation medium (1% FBS-HI, 1× ITS, 100 U/ml of penicillin and 100 µg/ml of streptomycin in DMEM) supplemented with: 50 µg/ml L-ascorbic acid and 1 nM FGF2; 1 nM FGF2 and 0.1 µM BGJ398; 0.1 µM BGJ398; 10% FBS; or 10% FBS and 0.5 µM BGJ398. All treatments were carried out in intraexperimental duplicates or triplicates. The cells were cultured for 3 and 7 days. Fresh L-ascorbic acid was added to the cultures every 2 days. Fresh medium was added to the cultures after 3 days.

For detection of fibrous collagen, the fibroblast cultures were washed with PBS, fixed with Bouin's solution (75 ml of saturated picric acid solution, 25 ml of 40% formaldehyde, 5 ml of glacial acetic acid) for 1 h, washed with tap water and incubated for 1.5 h in 0.1% (w/v) Sirius Red (Merck) in saturated picric acid solution with mild shaking. After discarding the stain, the cell cultures were washed with 0.01 M HCl to remove unbound dye, dried and photographed using a Leica M165 FC stereo microscope equipped with a Leica DFC450C camera. Subsequently the bound dye was eluted using 0.1 M NaOH, extracts were collected, clarified by centrifugation (10,000 g) and their absorbance at 550 nm was measured using a Synergy HTX reader (Bio-Tek).

For the detection of glycosaminoglycans, the fibroblast cultures were washed with PBS and fixed with 4% formaldehyde (Bio-Optica) for 1 h at 4°C. After washing with 0.1 M HCl, the cultures were incubated with 0.5% Alcian Blue 8GX (Serva) in 0.1 M HCl. Afterwards, the staining solution was discarded and the cultures were extensively washed with deionized water to remove any unbound stain. The cultures were scraped into 1% SDS to extract bound dye, centrifuged (10,000 g) and the absorbance of the supernatant at 350 nm was measured using a Synergy HTX reader.

For the quantification of cell number, the medium was removed and fibroblast cultures were supplied with 10 µg/ml resazurin in DMEM and the plates were incubated for 3 h at 37°C, 5% CO₂, followed by measurement of resorufin fluorescence using a Synergy H4 Hybrid multi-mode microplate reader.

Production of cell-derived matrices

Fibroblasts were cultured on gelatin-coated coverslips to full confluence, then washed three times with PBS and treated with ECM starvation medium (1% FBS-HI, 1× ITS, 100 U/ml of penicillin and 100 µg/ml of streptomycin in DMEM) with no FGF, 1 nM FGF2 or 10% FBS, and supplemented with 50 µg/ml L-ascorbic acid (Merck). The cells were cultured for 11 days and the medium was changed every day. After 11 days of cultivation, the cultures were decellularized according to published protocol (Kaukonen et al., 2017) and processed for scanning electron microscopy.

Scanning electron microscopy

The samples were fixed with 3% glutaraldehyde in 100 mM sodium cacodylate buffer (pH 7.4) for 45 min, washed with cacodylate buffer and dehydrated in an ethanol series. Samples were dried in the CPD 030 critical

point dryer (Bal-Tec) and then sputter-coated with gold using the SCD 040 (Balzers Union) at 30 mA for 3 min. Gilded specimens were analyzed with a scanning electron microscope Vega TS 5136 XM (Tescan).

Real-time quantitative PCR (qPCR)

RNA from fibroblasts was isolated using the RNeasy Mini Kit (Qiagen) according to the manufacturer's instructions. RNA concentration was measured using the NanoDrop 2000 (Thermo Fisher Scientific). RNA was transcribed into cDNA using the Transcriptor First Strand cDNA Synthesis Kit (Roche) or TaqMan Reverse Transcription kit (Life Technologies). Real-time qPCR was performed using 5 ng cDNA, 5 pmol each of the forward and reverse gene-specific primers (primer sequences are shown in Table S3) in the Light Cycler SYBR Green I Master mix (Roche) on a LightCycler 480 II (Roche). Relative gene expression was calculated using the $\Delta\Delta C_t$ method and normalization to two housekeeping genes, β -actin (*Actb*) and eukaryotic elongation factor 1 γ (*Eef1g*).

Collagen contraction assay

Fibroblasts were collected from cell culture dishes by trypsinization, washed three times with PBS to remove any traces of serum and suspended in DMEM. Neutralized collagen was prepared by combining 12.5 volumes of collagen type I (Corning) with 1 volume of 0.22 M NaOH, 5 \times collagen reconstitution buffer (5 \times MEM, 20 μ g/ml NaHCO₃, 0.1 M HEPES), DMEM and fibroblast suspension to the final concentration of 2.58 mg/ml collagen, 1 \times MEM, and a final cell density of 2.8 \times 10⁵ cell/ml. Equal volumes of the collagen-fibroblast mixture were plated in 24-well BSA-coated plates (712 μ l/well) and incubated at 37°C, 5% CO₂ for 1 h before medium (1 \times ITS, 100 U/ml of penicillin and 100 μ g/ml of streptomycin in DMEM) with 5 nM FGF ligands and/or inhibitors, as required for the experiment, was added on the top. The gels were cultured for 2 days and fixed using neutral buffered formalin. Fixed gels were photographed using a Leica M165 FC microscope equipped with a Leica DFC450C camera. The images were merged using Adobe Photoshop and the gel area was measured in ImageJ. The extent of gel contraction was calculated as the percentage of the area of a non-contracted gel with no cells.

3D culture of mammary organoids and fibroblasts

3D culture of mammary organoids and fibroblasts was performed as previously described (Koledova and Lu, 2017). Briefly, the freshly isolated mammary organoids were embedded in growth factor-reduced Matrigel either alone or with mammary fibroblasts and plated in domes. After setting the gel for 45–60 min at 37°C, the cultures were overlaid with basal organoid medium (1 \times ITS, 100 U/ml of penicillin and 100 μ g/ml of streptomycin in DMEM/F12), supplied with 1 nM FGF2 (Peprotech) or 50 μ g/ml protamine sulfate (Merck) according to the experiment. The cultures were incubated in a humidified atmosphere of 5% CO₂ at 37°C on an Olympus IX81 microscope equipped with a Hamamatsu camera and CellR system for time-lapse imaging. The organoids were photographed every 60 min for 5 days with manual refocusing every day. The images were exported and analyzed using ImageJ. Organoid branching was evaluated from videos and it was defined as the formation of a new bud and/or branch from the organoid. Organoids that fused with another organoid or collapsed after attachment to the bottom of the dish were excluded from the quantification.

Growth factor production in the 3D (co-)cultures was analyzed on day 3 from the media using mouse growth factor array (Ray Biotech) and from cell lysates using qPCR. For qPCR analysis of *Fgf2* expression in response to FGF2 in fibroblasts, the fibroblasts were cultured in 3D for 24 h in serum-starvation medium (1 \times ITS, 0.2% FBS, 100 U/ml of penicillin and 100 μ g/ml of streptomycin in DMEM) and then treated with 5 nM FGF2 and 4 μ g/ml heparin in serum-starvation medium for 24 h.

Knockdown of *Fgfr1/2* in mammary fibroblasts

The pre-designed Silencer Select siRNAs against *Fgfr1* (IDs s66023 and s66025) and *Fgfr2* (IDs s66028 and s201348) and the scrambled negative control siRNA were ordered from Thermo Fisher Scientific. Transfection was performed with Lipofectamine 3000 Reagent (Thermo Fisher Scientific) according to the manufacturer's instructions at 20 nM siRNA. Transfection efficiency was determined by qPCR analysis of

Fgfr1c and *Fgfr2c* mRNA levels, normalized to housekeeping genes *Actb* and *Eef1g*.

Statistical analysis

Statistical analysis was performed using GraphPad Prism software. The Student's *t*-test (unpaired, two-tailed) was used for comparison of two groups. For comparison of three or more groups, one-way ANOVA was used when normality could be confirmed by the D'Agostino & Pearson omnibus normality test. The nonparametric Kruskal–Wallis test was used when non-normally distributed groups were compared or when normality could not be tested (owing to a too small data set). The Friedman test was used for matched data with non-Gaussian distribution. Bar plots were generated by GraphPad Prism and show mean \pm s.d. **P*<0.05, ***P*<0.01, ****P*<0.001, *****P*<0.0001. The number of independent biological replicates is indicated as *n*.

Acknowledgements

We thank Anas Rabata, Julia Smelkova, Denisa Belisova, Zuzana Garlikova, Michaela Klouckova and Katarina Mareckova for technical assistance, Josef Jaros for providing a tool for image data processing and Jakub Cernek for help with image analysis. We acknowledge the Cellular Imaging Core Facility of the Central European Institute of Technology, supported by the Czech-Biomed large RI project (LM2015062 funded by the Ministry of Education, Youth and Sport of the Czech Republic) for their support with obtaining scientific data presented in this paper.

Competing interests

The authors declare no competing or financial interests.

Author contributions

Conceptualization: Z.K.; Methodology: Z.K.; Investigation: Z.K., J.S.; Resources: Z.K.; Writing - original draft: Z.K.; Writing - review & editing: Z.K., J.S.; Supervision: Z.K.; Project administration: Z.K.; Funding acquisition: Z.K.

Funding

This study was supported by the Grantová Agentura České Republiky [GJ16-20031Y to Z.K.]; the Grant Agency of Masarykova Univerzita [MUNI/E/0519/2019 to Z.K.]; and by funds from the Lékařská fakulta, Masarykova Univerzita to junior researcher Z.K. [ROZV/24/2018].

Supplementary information

Supplementary information available online at <http://dev.biologists.org/lookup/doi/10.1242/dev.185306.supplemental>

References

- Affolter, M., Zeller, R. and Caussinus, E. (2009). Tissue remodelling through branching morphogenesis. *Nat. Rev. Mol. Cell Biol.* **10**, 831–842. doi:10.1038/nrm2797
- Ahn, S., Cho, J., Sung, J., Lee, J. E., Nam, S. J., Kim, K.-M. and Cho, E. Y. (2012). The prognostic significance of tumor-associated stroma in invasive breast carcinoma. *Tumour Biol.* **33**, 1573–1580. doi:10.1007/s13277-012-0411-6
- Bernard, S., Myers, M., Fang, W. B., Zinda, B., Smart, C., Lambert, D., Zou, A., Fan, F. and Cheng, N. (2018). CXCL1 derived from mammary fibroblasts promotes progression of mammary lesions to invasive carcinoma through CXCR2 dependent mechanisms. *J. Mammary Gland Biol. Neoplasia* **23**, 249–267. doi:10.1007/s10911-018-9407-1
- Bernfield, M., Götte, M., Park, P. W., Reizes, O., Fitzgerald, M. L., Lincecum, J. and Zako, M. (1999). Functions of cell surface heparan sulfate proteoglycans. *Annu. Rev. Biochem.* **68**, 729–777. doi:10.1146/annurev.biochem.68.1.729
- Bonnans, C., Chou, J. and Werb, Z. (2014). Remodelling the extracellular matrix in development and disease. *Nat. Rev. Mol. Cell Biol.* **15**, 786. doi:10.1038/nrm3904
- Brownfield, D. G., Venugopalan, G., Lo, A., Mori, H., Tanner, K., Fletcher, D. A. and Bissell, M. J. (2013). Patterned collagen fibers orient branching mammary epithelium through distinct signaling modules. *Curr. Biol.* **23**, 703–709. doi:10.1016/j.cub.2013.03.032
- Chakravarthy, A., Khan, L., Bensler, N. P., Bose, P. and De Carvalho, D. D. (2018). TGF- β -associated extracellular matrix genes link cancer-associated fibroblasts to immune evasion and immunotherapy failure. *Nat. Commun.* **9**, 4692. doi:10.1038/s41467-018-06654-8
- Chioni, A.-M. and Grose, R. (2012). FGFR1 cleavage and nuclear translocation regulates breast cancer cell behavior. *J. Cell Biol.* **197**, 801–817. doi:10.1083/jcb.201108077

- Ciarloni, L., Mallepell, S. and Briskens, C. (2007). Amphiregulin is an essential mediator of estrogen receptor alpha function in mammary gland development. *Proc. Natl. Acad. Sci. USA* **104**, 5455-5460. doi:10.1073/pnas.0611647104
- Cid, S., Eiro, N., Fernández, B., Sánchez, R., Andicoechea, A., Fernández-Muñiz, P. I., González, L. O. and Vizoso, F. J. (2018). Prognostic influence of tumor stroma on breast cancer subtypes. *Clin. Breast Cancer* **18**, e123-e133. doi:10.1016/j.clbc.2017.08.008
- Ewald, A. J., Brenot, A., Duong, M., Chan, B. S. and Werb, Z. (2008). Collective epithelial migration and cell rearrangements drive mammary branching morphogenesis. *Dev. Cell* **14**, 570-581. doi:10.1016/j.devcel.2008.03.003
- Fata, J. E., Mori, H., Ewald, A. J., Zhang, H., Yao, E., Werb, Z. and Bissell, M. J. (2007). The MAPK^{ERK1-2} pathway integrates distinct and antagonistic signals from TGF α and FGF7 in morphogenesis of mouse mammary epithelium. *Dev. Biol.* **306**, 193-207. doi:10.1016/j.ydbio.2007.03.013
- Feinberg, T. Y., Zheng, H., Liu, R., Wicha, M. S., Yu, S. M. and Weiss, S. J. (2018). Divergent matrix-remodeling strategies distinguish developmental from neoplastic mammary epithelial cell invasion programs. *Dev. Cell* **47**, 145-160.e6. doi:10.1016/j.devcel.2018.08.025
- Finak, G., Bertos, N., Pepin, F., Sadekova, S., Souleimanova, M., Zhao, H., Chen, H., Omeroglu, G., Meterissian, S., Omeroglu, A. et al. (2008). Stromal gene expression predicts clinical outcome in breast cancer. *Nat. Med.* **14**, 518-527. doi:10.1038/nm1764
- Forsten-Williams, K., Chu, C. L., Fannon, M., Buczek-Thomas, J. A. and Nugent, M. A. (2008). Control of growth factor networks by heparan sulfate proteoglycans. *Ann. Biomed. Eng.* **36**, 2134-2148. doi:10.1007/s10439-008-9575-z
- Francavilla, C., Rigbolt, K. T. G., Emdal, K. B., Carraro, G., Vernet, E., Bekker-Jensen, D. B., Streicher, W., Wikström, M., Sundström, M., Bellusci, S. et al. (2013). Functional proteomics defines the molecular switch underlying FGF receptor trafficking and cellular outputs. *Mol. Cell* **51**, 707-722. doi:10.1016/j.molcel.2013.08.002
- Gaggioli, C., Hooper, S., Hidalgo-Carcedo, C., Grosse, R., Marshall, J. F., Harrington, K. and Sahai, E. (2007). Fibroblast-led collective invasion of carcinoma cells with differing roles for RhoGTPases in leading and following cells. *Nat. Cell Biol.* **9**, 1392-1400. doi:10.1038/ncb1658
- Garner, O. B., Bush, K. T., Nigam, K. B., Yamaguchi, Y., Xu, D., Esko, J. D. and Nigam, S. K. (2011). Stage-dependent regulation of mammary ductal branching by Heparan sulfate and HGF-cMet signaling. *Dev. Biol.* **355**, 394-403. doi:10.1016/j.ydbio.2011.04.035
- Gastaldi, S., Sassi, F., Accornero, P., Torti, D., Galimi, F., Migliardi, G., Molyneux, G., Perera, T., Comoglio, P. M., Boccaccio, C. et al. (2013). Met signaling regulates growth, repopulating potential and basal cell-fate commitment of mammary luminal progenitors: implications for basal-like breast cancer. *Oncogene* **32**, 1428-1440. doi:10.1038/ncr.2012.154
- Grinnell, F. (2000). Fibroblast-collagen-matrix contraction: growth-factor signalling and mechanical loading. *Trends Cell Biol.* **10**, 362-365. doi:10.1016/S0962-8924(00)01802-X
- Grinnell, F. and Petroll, W. M. (2010). Cell motility and mechanics in three-dimensional collagen matrices. *Annu. Rev. Cell Dev. Biol.* **26**, 335-361. doi:10.1146/annurev.cellbio.042308.113318
- Guagnano, V., Furet, P., Spanka, C., Bordas, V., Le Douget, M., Stamm, C., Brueggen, J., Jensen, M. R., Schnell, C., Schmid, H. et al. (2011). Discovery of 3-(2,6-dichloro-3,5-dimethoxy-phenyl)-1-(6-[4-(4-ethyl-piperazin-1-yl)-phenylamino]-pyrimidin-4-yl)-1-methyl-urea (NVP-BGJ398), a potent and selective inhibitor of the fibroblast growth factor receptor family of receptor tyrosine kinase. *J. Med. Chem.* **54**, 7066-7083. doi:10.1021/jm2006222
- Hammer, A. M., Sizemore, G. M., Shukla, V. C., Avendano, A., Sizemore, S. T., Chang, J. J., Kladney, R. D., Cuitiño, M. C., Thies, K. A., Verfurth, Q. et al. (2017). Stromal PDGFR α activation enhances matrix stiffness, impedes mammary ductal development, and accelerates tumor growth. *Neoplasia* **19**, 496-508. doi:10.1016/j.neo.2017.04.004
- Haslam, S. Z. (1986). Mammary fibroblast influence on normal mouse mammary epithelial cell responses to estrogen in vitro. *Cancer Res.* **46**, 310-316.
- Hovey, R. C., Trott, J. F. and Vonderhaar, B. K. (2002). Establishing a framework for the functional mammary gland: from endocrinology to morphology. *J. Mammary Gland Biol. Neoplasia* **7**, 17-38. doi:10.1023/A:101576632258
- Ingman, W. V., Wyckoff, J., Gouon-Evans, V., Condeelis, J. and Pollard, J. W. (2006). Macrophages promote collagen fibrillogenesis around terminal end buds of the developing mammary gland. *Dev. Dyn.* **235**, 3222-3229. doi:10.1002/dvdy.20972
- Jones, C. E., Hammer, A. M., Cho, Y. J., Sizemore, G. M., Cukierman, E., Yee, L. D., Ghadiali, S. N., Ostrowski, M. C. and Leight, J. L. (2019). Stromal PTEN regulates extracellular matrix organization in the mammary gland. *Neoplasia* **21**, 132-145. doi:10.1016/j.neo.2018.10.010
- Kalluri, R. and Zeisberg, M. (2006). Fibroblasts in cancer. *Nat. Rev. Cancer* **6**, 392-401. doi:10.1038/nrc1877
- Kaukonen, R., Jacquemet, G., Hamidi, H. and Ivaska, J. (2017). Cell-derived matrices for studying cell proliferation and directional migration in a complex 3D microenvironment. *Nat. Protoc.* **12**, 2376-2390. doi:10.1038/nprot.2017.107
- Kettunen, P., Karavanova, I. and Thesleff, I. (1998). Responsiveness of developing dental tissues to fibroblast growth factors: expression of splicing alternatives of FGFR1, -2, -3, and of FGFR4; and stimulation of cell proliferation by FGF-2, -4, -8, and -9. *Dev. Genet.* **22**, 374-385. doi:10.1002/(SICI)1520-6408(1998)22:4<374::AID-DVG7>3.0.CO;2-3
- Kim, E.-J., Jung, H.-S. and Lu, P. (2013). Pleiotropic functions of fibroblast growth factor signaling in embryonic mammary gland development. *J. Mammary Gland Biol. Neoplasia* **18**, 139-142. doi:10.1007/s10911-013-9278-4
- Ko, M. H. K. and Kay, E. D. P. (2005). Regulatory role of FGF-2 on type I collagen expression during endothelial mesenchymal transformation. *Invest. Ophthalmol. Vis. Sci.* **46**, 4495-4503. doi:10.1167/iovs.05-0818
- Koledova, Z. (2017). 3D coculture of mammary organoids with fibrospheres: a model for studying epithelial-stromal interactions during mammary branching morphogenesis. *Methods Mol. Biol.* **1612**, 107-124. doi:10.1007/978-1-4939-7021-6_8
- Koledova, Z. and Lu, P. (2017). A 3D fibroblast-epithelium co-culture model for understanding microenvironmental role in branching morphogenesis of the mammary gland. *Methods Mol. Biol.* **1501**, 217-231. doi:10.1007/978-1-4939-6475-8_10
- Koledova, Z., Zhang, X., Streuli, C., Clarke, R. B., Klein, O. D., Werb, Z. and Lu, P. (2016). SPRY1 regulates mammary epithelial morphogenesis by modulating EGFR-dependent stromal paracrine signaling and ECM remodeling. *Proc. Natl. Acad. Sci. USA* **113**, E5731-E5740. doi:10.1073/pnas.1611532113
- Krause, S., Maffini, M. V., Soto, A. M. and Sonnenschein, C. (2008). A novel 3D in vitro culture model to study stromal-epithelial interactions in the mammary gland. *Tissue Eng. Part C Methods* **14**, 261-271. doi:10.1089/ten.tec.2008.0030
- Kuperwasser, C., Chavarria, T., Wu, M., Magrane, G., Gray, J. W., Carey, L., Richardson, A. and Weinberg, R. A. (2004). Reconstruction of functionally normal and malignant human breast tissues in mice. *Proc. Natl. Acad. Sci. USA* **101**, 4966-4971. doi:10.1073/pnas.0401064101
- Liu, Y.-J., Le Berre, M., Lautenschlaeger, F., Maiuri, P., Callan-Jones, A., Heuzé, M., Takaki, T., Voituriez, R. and Piel, M. (2015). Confinement and low adhesion induce fast amoeboid migration of slow mesenchymal cells. *Cell* **160**, 659-672. doi:10.1016/j.cell.2015.01.007
- Lu, P. and Werb, Z. (2008). Patterning mechanisms of branched organs. *Science* **322**, 1506-1509. doi:10.1126/science.1162783
- Lu, P., Ewald, A. J., Martin, G. R. and Werb, Z. (2008). Genetic mosaic analysis reveals FGF receptor 2 function in terminal end buds during mammary gland branching morphogenesis. *Dev. Biol.* **321**, 77-87. doi:10.1016/j.ydbio.2008.06.005
- Maddaluno, L., Urwyler, C. and Werner, S. (2017). Fibroblast growth factors: key players in regeneration and tissue repair. *Development* **144**, 4047-4060. doi:10.1242/dev.152587
- Mailleux, A. A., Spencer-Dene, B., Dillon, C., Ndiaye, D., Savona-Baron, C., Itoh, N., Kato, S., Dickson, C., Thiery, J. P. and Bellusci, S. (2002). Role of FGF10/FGFR2b signaling during mammary gland development in the mouse embryo. *Development* **129**, 53-60.
- Morsing, M., Klitgaard, M. C., Jafari, A., Villadsen, R., Kassem, M., Petersen, O. W. and Rønnow-Jessen, L. (2016). Evidence of two distinct functionally specialized fibroblast lineages in breast stroma. *Breast Cancer Res.* **18**, 108. doi:10.1186/s13058-016-0769-2
- Moses, H. and Barcellos-Hoff, M. H. (2011). TGF- β biology in mammary development and breast cancer. *Cold Spring Harb. Perspect. Biol.* **3**, a003277. doi:10.1101/cshperspect.a003277
- Mundhenke, C., Meyer, K., Drew, S. and Friedl, A. (2002). Heparan sulfate proteoglycans as regulators of fibroblast growth factor-2 receptor binding in breast carcinomas. *Am. J. Pathol.* **160**, 185-194. doi:10.1016/S0002-9440(10)64362-3
- Nelson, C. M. and Bissell, M. J. (2006). Of extracellular matrix, scaffolds, and signaling: tissue architecture regulates development, homeostasis, and cancer. *Annu. Rev. Cell Dev. Biol.* **22**, 287-309. doi:10.1146/annurev.cellbio.22.010305.104315
- Orimo, A., Gupta, P. B., SgROI, D. C., Arenzana-Seisdedos, F., Delaunay, T., Naeem, R., Carey, V. J., Richardson, A. L. and Weinberg, R. A. (2005). Stromal fibroblasts present in invasive human breast carcinomas promote tumor growth and angiogenesis through elevated SDF-1/CXCL12 secretion. *Cell* **121**, 335-348. doi:10.1016/j.cell.2005.02.034
- Ornitz, D. M. and Itoh, N. (2015). The fibroblast growth factor signaling pathway. *Wiley Interdiscip. Rev. Dev. Biol.* **4**, 215-266. doi:10.1002/wdev.176
- Orr-Urtreger, A., Bedford, M. T., Burakova, T., Arman, E., Zimmer, Y., Yayon, A., Givol, D. and Lonai, P. (1993). Developmental localization of the splicing alternatives of fibroblast growth factor receptor-2 (FGFR2). *Dev. Biol.* **158**, 475-486. doi:10.1006/dbio.1993.1205
- Parsa, S., Ramasamy, S. K., De Langhe, S., Gupte, V. V., Haigh, J. J., Medina, D. and Bellusci, S. (2008). Terminal end bud maintenance in mammary gland is dependent upon FGFR2b signaling. *Dev. Biol.* **317**, 121-131. doi:10.1016/j.ydbio.2008.02.014
- Pavlovich, A. L., Manivannan, S. and Nelson, C. M. (2010). Adipose stroma induces branching morphogenesis of engineered epithelial tubules. *Tissue Eng. Part A* **16**, 3719-3726. doi:10.1089/ten.tea.2009.0836
- Peuhu, E., Kaukonen, R., Lerche, M., Saari, M., Guzmán, C., Rantakari, P., De Franceschi, N., Wärrri, A., Georgiadou, M., Jacquemet, G. et al. (2017).

- SHARPIN regulates collagen architecture and ductal outgrowth in the developing mouse mammary gland. *EMBO J.* **36**, 165-182. doi:10.15252/embj.201694387
- Polyak, K. and Kalluri, R.** (2010). The role of the microenvironment in mammary gland development and cancer. *Cold Spring Harb. Perspect. Biol.* **2**, a003244. doi:10.1101/cshperspect.a003244
- Pond, A. C., Bin, X., Batts, T., Roarty, K., Hilsenbeck, S. and Rosen, J. M.** (2013). Fibroblast growth factor receptor signaling is essential for normal mammary gland development and stem cell function. *Stem Cells* **31**, 178-189. doi:10.1002/stem.1266
- Relf, M., LeJeune, S., Scott, P. A., Fox, S., Smith, K., Leek, R., Moghaddam, A., Whitehouse, R., Bicknell, R. and Harris, A. L.** (1997). Expression of the angiogenic factors vascular endothelial cell growth factor, acidic and basic fibroblast growth factor, tumor growth factor beta-1, platelet-derived endothelial cell growth factor, placenta growth factor, and pleiotrophin in human primary breast cancer and its relation to angiogenesis. *Cancer Res.* **57**, 963-969.
- Rice, D. P. C., Rice, R. and Thesleff, I.** (2003). Fgfr mRNA isoforms in craniofacial bone development. *Bone* **33**, 14-27. doi:10.1016/S8756-3282(03)00163-7
- Schedin, P. and Hovey, R. C.** (2010). Editorial: the mammary stroma in normal development and function. *J. Mammary Gland Biol. Neoplasia* **15**, 275-277. doi:10.1007/s10911-010-9191-z
- Schedin, P. and Keely, P. J.** (2011). Mammary gland ECM remodeling, stiffness, and mechanosignaling in normal development and tumor progression. *Cold Spring Harb. Perspect. Biol.* **3**, a003228. doi:10.1101/cshperspect.a003228
- Shi, H.-X., Lin, C., Lin, B.-B., Wang, Z.-G., Zhang, H.-Y., Wu, F.-Z., Cheng, Y., Xiang, L.-J., Guo, D.-J., Luo, X. et al.** (2013). The anti-scar effects of basic fibroblast growth factor on the wound repair in vitro and in vivo. *PLoS ONE* **8**, e59966. doi:10.1371/journal.pone.0059966
- Silberstein, G. B. and Daniel, C. W.** (1987). Reversible inhibition of mammary gland growth by transforming growth factor-beta. *Science* **237**, 291-293. doi:10.1126/science.3474783
- Sit, S.-T. and Manser, E.** (2011). Rho GTPases and their role in organizing the actin cytoskeleton. *J. Cell Sci.* **124**, 679-683. doi:10.1242/jcs.064964
- Sternlicht, M. D., Sunnarborg, S. W., Kouros-Mehr, H., Yu, Y., Lee, D. C. and Werb, Z.** (2005). Mammary ductal morphogenesis requires paracrine activation of stromal EGFR via ADAM17-dependent shedding of epithelial amphiregulin. *Development* **132**, 3923-3933. doi:10.1242/dev.01966
- Suga, H., Eto, H., Shigeura, T., Inoue, K., Aoi, N., Kato, H., Nishimura, S., Manabe, I., Gonda, K. and Yoshimura, K.** (2009). IFATS collection: Fibroblast growth factor-2-induced hepatocyte growth factor secretion by adipose-derived stromal cells inhibits postinjury fibrogenesis through a c-Jun N-terminal kinase-dependent mechanism. *Stem Cells* **27**, 238-249. doi:10.1634/stemcells.2008-0261
- Sun, L., Tran, N., Liang, C., Tang, F., Rice, A., Schreck, R., Waltz, K., Shawver, L. K., McMahon, G. and Tang, C.** (1999). Design, synthesis, and evaluations of substituted 3-[(3- or 4-carboxyethylpyrrol-2-yl)methylidene]indolin-2-ones as inhibitors of VEGF, FGF, and PDGF receptor tyrosine kinases. *J. Med. Chem.* **42**, 5120-5130. doi:10.1021/jm9904295
- Totsukawa, G., Wu, Y., Sasaki, Y., Hartshorne, D. J., Yamakita, Y., Yamashiro, S. and Matsumura, F.** (2004). Distinct roles of MLCK and ROCK in the regulation of membrane protrusions and focal adhesion dynamics during cell migration of fibroblasts. *J. Cell Biol.* **164**, 427. doi:10.1083/jcb.200306172
- Tschumperlin, D. J.** (2013). Fibroblasts and the ground they walk on. *Physiology (Bethesda)* **28**, 380-390. doi:10.1152/physiol.00024.2013
- Turner, N. and Grose, R.** (2010). Fibroblast growth factor signalling: from development to cancer. *Nat. Rev. Cancer* **10**, 116-129. doi:10.1038/nrc2780
- Wiseman, B. S. and Werb, Z.** (2002). Stromal effects on mammary gland development and breast cancer. *Science* **296**, 1046-1049. doi:10.1126/science.1067431
- Wolzt, M., Weltermann, A., Nieszpauro-Los, M., Schneider, B., Fassolt, A., Lechner, K., Eichler, H. G. and Kyrle, P. A.** (1995). Studies on the neutralizing effects of protamine on unfractionated and low molecular weight heparin (Fragmin) at the site of activation of the coagulation system in man. *Thromb. Haemost.* **73**, 439-443. doi:10.1055/s-0038-1653794
- Yamagishi, M. and Okamoto, H.** (2010). Competition for ligands between FGFR1 and FGFR4 regulates Xenopus neural development. *Int. J. Dev. Biol.* **54**, 93-104. doi:10.1387/ijdb.092849my
- Zhang, H.-Z., Bennett, J. M., Smith, K. T., Sunil, N. and Haslam, S. Z.** (2002). Estrogen mediates mammary epithelial cell proliferation in serum-free culture indirectly via mammary stroma-derived hepatocyte growth factor. *Endocrinology* **143**, 3427-3434. doi:10.1210/en.2002-220007
- Zhang, X., Qiao, G. and Lu, P.** (2014a). Modulation of fibroblast growth factor signaling is essential for mammary epithelial morphogenesis. *PLoS ONE* **9**, e92735. doi:10.1371/journal.pone.0092735
- Zhang, X., Martinez, D., Koledova, Z., Qiao, G., Streuli, C. H. and Lu, P.** (2014b). FGF ligands of the postnatal mammary stroma regulate distinct aspects of epithelial morphogenesis. *Development* **141**, 3352-3362. doi:10.1242/dev.106732
- Zhu, H., Duchesne, L., Rudland, P. S. and Fernig, D. G.** (2010). The heparan sulfate co-receptor and the concentration of fibroblast growth factor-2 independently elicit different signalling patterns from the fibroblast growth factor receptor. *Cell Commun. Signal.* **8**, 14. doi:10.1186/1478-811X-8-14